Seismic and Volcanic Hazard Analysis for Mount Cameroon Volcano

By

ARIANE WETIE NGONGANG

University of Pretoria

Submitted in partial fulfilment of the requirements for the degree of

MASTER OF SCIENCE (MSc) IN GEOLOGY

Department of Geology in the Faculty of

Natural and Agricultural Sciences at the

University of Pretoria

Pretoria

2016

Supervisors: Professor A. Kijko

Co. Supervisor: Doctor N. Lenhardt

DECLARATION

I, Ariane Wetie Ngongang, declare that the dissertation, submitted for the degree of Master of Science in Geology at the University of Pretoria, is my own work and has not been previously been submitted by me for a degree purpose at this or any other tertiary institution.

SIGNATURE:

DATE: ……19 December 2016……

This dissertation is dedicated to my Fiancé

Marius Tchonang and daughter Sharleen Tchonang

ACKNOWLEDGEMENTS

"Better the end of a thing than the beginning". It has been an incredible long academic journey where a lot of skills and knowledge that would see me through my entire life have been acquired. All this would have never been feasible without academic, financial and moral support from the following people.

First of all, I would like to express my deepest gratitude to my supervisor Prof. Andrzej Kijko for the last minute financial intervention to bring this project forward. I would also wish to thank him for his constant support for the past three years. Prof, your willingness to provide all the material and technical support I needed and your constant encouragement and advices made it possible for me to realise this achievement.

Equally, I would like to thank my co-supervisor: Dr. Nils Lenhardt for his tremendous contribution. All your time spent in reading my manuscripts and coming up with great ideas on how to modify and restructure it are greatly appreciated. Working with you has been an amazing experience. Our constant academic interaction with your eagerness for perfection has pushed me to go extra miles in understanding the concepts presented in this dissertation. Thank you for your patience. One simply could not wish for a better or friendlier supervisor.

For the acquisition of GIS skills that represented a very important part of this work, I wish to thank Ms Sukanya Lenhardt for her kind assistance. You were always ready to create time from your busy schedule to help me out when I was blocked and needed some guidance. I would like to thank you for the considerable good job in coming up with relevant techniques that I needed to advance with my research and bring it up to the standard presented in this dissertation.

Most importantly, none of this would have been possible without the love, advice and patience of my family, to whom this dissertation is dedicated to. Mr. Marius Tchonang , you have been a constant source of love, concern, support and strength all these years. For that, I will always be indebted to you.

Even though their role might have appeared insignificant, there are a few people that were indispensable to the realisation of this study.

I am endlessly grateful to my family and friends whose constant love, prayers and moral support surpassed all the academics hardship I experience throughout this work. To my late mother Martine Tchakeu who even though never saw this day in person, would have been so proud of my achievements. May your soul rest in peace mum. Special thanks to my dad Jean-Pierre Ngongang, whose love for education made me attain this level. Many thanks to my brothers, Christian Nganwa and Alex Kouaghu for their encouragement and support. I would like to

thank Dr. Alain Tokam, who as a good friend was always willing to help and give his best suggestions. I would also like to thank all those that I forgot to mention and who showed interest and assisted me in one way or the other in the past three years.

Finally to God Almighty, who gave me strength, wisdom and provided manpower that I needed in the realisation of this work. To Him be the Glory for ever and ever.

ABSTRACT

Mount Cameroon is considered the only active volcano along a 1600 km long chain of volcanic complexes called the Cameroon Volcanic Line (CVL). It has erupted seven times during the last 100 years, the most recent was in May 2000. The approximately 500,000 inhabitants that live and work around the fertile flanks are exposed to impending threats from volcanic eruptions and earthquakes.

In this thesis, a hazard assessment study that involves both statistical modelling of seismic hazard parameters and the evaluation of a future volcanic risk was undertaken on Mount Cameroon. The Gutenberg-Richter magnitude-frequency relations, the annual activity rate, the maximum magnitude, the rate of volcanic eruptions and risks assessment were examined.

The seismic hazard parameters were estimated using the Maximum Likelihood Method on the basis of a procedure which combines seismic data containing incomplete files of large historical events with complete files of short periods of observations. A homogenous Poisson distribution model was applied to previous recorded volcanic eruptions of Mount Cameroon to determine the frequency of eruption and assess the probability of a future eruption.

Frequency-magnitude plots indicated that Gutenberg-Richter *b*-values are partially dependent on the maximum regional magnitude and the method used in their calculation. *b*-values showed temporal and spatial variation with an average value of 1.53 ± 0.02. The intrusion of a magma body generating the occurrence of relatively small earthquakes as observed in our instrumental catalogue, could be responsible for this high anomalous *b*-value.

An epicentre map of locally recorded earthquakes revealed that the southeastern zone is the most seismically active part of the volcano. The annual mean activity rate of the seismicity strongly depends on the time span of the seismic catalogue and results showed that on average, one earthquake event occurs every 10 days. The maximum regional magnitude values which had been determined from various approaches overlap when their standard deviations are taken into account. However, the magnitude distribution model of the Mt. Cameroon earthquakes might not follow the form of the Gutenberg-Richter frequency magnitude relationship.

The datations of the last eruptive events that have occurred on Mt. Cameroon volcanic complex are presented. No specific pattern was observed on the frequency of eruptions, which means that a homogenous Poisson distribution provides a suitable model to estimate the rate of occurrence of volcanic eruptions and evaluate the risk of a future eruption. Two different approaches were

used to estimate the mean eruption rate (λ) and both yielded a value of 0.074. The results showed that eruptions take place on average once every 13 years and, with the last eruption occurring over 15 years ago, it is considered that there is at present a high risk of an eruption to occur.

Keys words: Mount Cameroon, Seismic parameters, Poisson distribution, Rate of occurrence

LIST OF ABBREVIATIONS AND ACRONYMS

CAFB: Central African Fold Belt

CASZ: Central African Shear Zone

CDF: Cumulative Distribution Function

CVL: Cameroon Volcanic Line

FMD: Frequency Magnitude Distribution

FSZ: Foumban Shear Zone

G-R: Gutenberg Richter

K-S: Kijko-Sellevoll

K-S-B: Kijko-Sellevoll-Bayes

MLE: Maximum Likelihood Estimation

m_{max} :maximum possible earthquake

Mt. Cameroon: Mount Cameroon

NE: northeast

NNE: north-northwest

N-P-G: Non-parametric with Gaussian Kernel

NW: northwest

PDF: Probability Density Function

PSHA: Probabilistic Seismic Hazard Assessment

SE: southeast

SSW: south-southwest

SW: southwest

TABLE OF CONTENT

LIST OF FIGURES

LIST OF TABLES

Chapter 1

Introduction and Background

1.1 Introduction

Detailed geophysical and geological knowledge of an active volcano is an important tool in hazards mitigation. Because volcanic eruptions can be very devastating in terms of human and economic costs, predicting the time, location and nature of future eruption is fundamental when it comes to volcanology. Volcanic activity is a natural disaster caused by the ascent of magma to the earth's surface and its eruption (Sparks, 2003). Numerous attempts to understand and predict these natural phenomena have yielded some fruitful results. Nevertheless, nature preserves its superiority over science by striking at places and times we expect the least. Seismicity monitoring is commonly used for short term volcanic forecasts since eruptions are often preceded by an increase in the number of earthquakes (Ambey et al., 1989).

In Cameroon, most felt earthquakes have been reported along the Cameroon Volcanic Line (CVL) and in coastal areas with numerous events coinciding with volcanic activities of the CVL (Tabod et al., 1992). However, large magnitude events (4.5 to 5 at the local scale) are not frequent within the CVL, suggesting that crustal stresses are often being released by small magnitude tremors as commonly observed in many volcanic provinces (Fairhead, 1985). The CVL, whose origin is still disputed, is a unique 1600 km line of volcanic complexes, striking N30°E, and is made up of an oceanic and a continental segment; thus, it is an important feature in Central Africa (Fitton, 1980; Moreau et al., 1987). Mount Cameroon (Mt.Cameroon), the highest of these volcanic centres, is located on the continental part midway along the CVL and recently erupted in 2000 (Suh et al., 2003, Fig. 1.2).

1.2 Motivation and objectives of the study

This thesis has two main objectives: (1) a probabilistic seismic hazard of the Mt. Cameroon volcanic region is assessed by determining the seismic hazard parameters and (2) a general statistical modelling of the historical recorded eruptions is applied to Mt. Cameroon volcano and the rate of volcanic eruptions, an important parameter of the Poisson probability model, is derived. The need to carry out a probabilistic hazard and risk assessment of Mt. Cameroon Volcano derives from the fact that it is currently the only active volcano of the CVL and its seismicity is by far the most important along that volcanic line (Tabod et al., 1992). Furthermore, since approximately 500,000 people are settled around the volcano (Njome et al., 2010), a future

volcanic activity may not only cause major economic losses, but could also result in high number of casualties and displacement of these people.

In order to achieve the objectives of this project, it was necessary to determine the basic seismic parameters such as the mean activity rate, the Gutenberg-Richter parameter, the level of completeness of each seismic catalogue and the maximum regional magnitude. Defining and understanding seismotectonic characteristics of a source zone is an important part of a seismic hazard analysis and requires the knowledge of the local and regional geology The probabilistic seismic hazard assessment (PSHA) is a computation of probabilities of occurrence of given levels of ground motion caused by earthquakes at a specific site per unit time (McGuire, 1993).

To calculate the level of ground motion, a catalogue of each seismic zone containing the location, size and depth of the occurred earthquakes is defined. Hypocenter depths of events used in this study were highly inaccurate with some events having uncertainties greater than 5 km whereas the deepest event is 55 km deep (Ambey, 1989). For that reason, the PSHA conducted in this study is limited to defining the principal seismic zones of Mt. Cameroon and producing hazard maps of the Mt. Cameroon region showing the probability of occurrence of future earthquakes with a given magnitude and within a given time period.

Statistical methods have been applied to various volcanoes to analyse the frequency of eruptions (Ho et al., 1991; Caniaux, 2005; Klein, 1982), and will be used as guidelines to estimate the probabilities of an eruption to occur on Mt. Cameroon in the next 50 years

The seismic activity of Mt. Cameroon is known for the past 100 years (historical seismicity), has been measured for the past 30 years (instrumental seismicity), and is currently monitored by the Geophysical and Volcanological Research Unit of Ekona (Thierry et al., 2008). The seismic catalogues used in this study contain local earthquakes generated at the level of the Mt Cameroon volcano from 1900 to 1991.

Such a study has not yet been done on Mt. Cameroon volcano, and is important for two main reasons: (1) hazard parameters were evaluated utilising as much as possible seismological information not only from the instrumental period, but also from the historic era and (2) a Poisson distribution function is selected as a good methodological test offering a suitable basis for risk assessment of future volcanic eruption. It was hoped that this study would improve our knowledge of the seismo-volcanic character of Mt. Cameroon, and could help in short term eruption forecasting.

1.3 Previous work

At present, most studies conducted in Cameroon focused on the geology and petrology of the predominant structures. A brief summary of the outcomes are highlighted in this section.

Lithological units of Cameroon consist of Precambrian basement, Cretaceous sedimentary rocks, Cenozoic sedimentary rocks and volcanic formations (Schlüter, 2008; Fig. 1.1). Precambrian rocks of the basement are formed of two stratigraphic units: the Central African Fold Belt (CAFB), which is alternatively called the Central African Shear Zone (CASZ) in the north, and an Archean core known as the Ntem Group in the south (Toteu et al., 2001; Fig. 1.1). The Ntem Group is situated in the northern part of the Congo Craton and formed about 2.9 Ga ago (Schlüter, 2008). This unit is largely composed of granite, gneiss and charnockite and is delineated in the west by the 2.1 Ga Nyong series metamorphic complexes (Toteu et al., 2001; Fig. 1.1). The CASZ is an important tectonic feature in central Africa and generally includes igneous and metamorphic Neoproterozoic rocks such as gneiss, schist, granites and migmatites intruded by quartz, diorite and granodiorites (Schlüter, 2008). In Cameroon, the CASZ extends from the Adamawa Plateau in the north through the SW where it is called the Foumban Shear Zone (FSZ) and then vanishes beneath the volcanic centres of the CVL (Tokam et al., 2010; Fig. 1.1).

Sedimentary formations are restricted in the south-western and the northern regions of the country. The Douala and Rio-del-Rey offshore sedimentary basins extend from Nigeria to southern Cameroon. They were formed during the opening of the equatorial Atlantic Ocean in Cretaceous-Miocene times (Moreau et al., 1987). In the north, Quaternary to Recent sediments are observed in the Lake Chad basin (Schlüter, 2008). The principal rock types of these formations are sandstones, conglomerates and shales.

The Cenozoic magmatic rocks, aged between 66 and 30 Ma can be divided into two main units: (1) the Ring complexes and (2) the volcanic centres of the CVL. The volcanic centres cross Cameroon in NE-SW direction and are believed to follow a major structural zone named the Foumban Shear Zone (Moreau et al., 1987; Fig. 1.1). More than 60 ring complexes from one to ten km in diameter crop out over a distance of 1000 km in the direction of the CVL (Schlüter, 2008). They correspond to volcanic-plutonic intrusions into the Pan-African basement and into the Cretaceous sediments (Deruelle et al., 1991).The principal rock types present in this stratigraphy are syenites and granites (Schlüter, 2008).

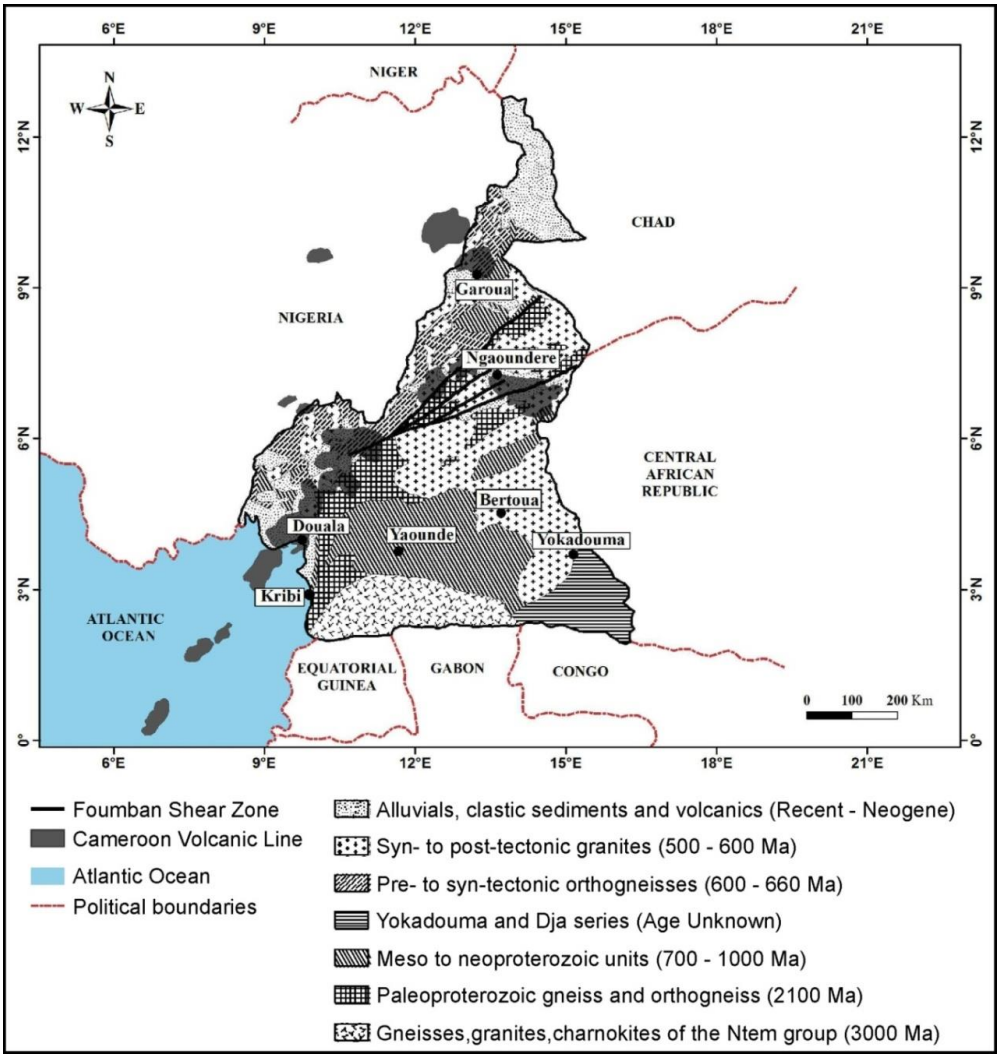

Figure 1.1: Geological setting of Cameroon showing the principal towns and the different types of rocks present with the corresponding age groups (modified after Toteu et al., 2001; Schlüter, 2008).

The CVL, also referred as Cameroon Line (Fitton, 1980; Moreau et al., 1987; Montigny et al., 2004) or Cameroon Hot Line (Deruelle et al., 2007) represents a 1600 km long line volcanic centres that have evolved into both oceanic and continental domains during the opening of the Atlantic Ocean (Deruelle et al., 1987; Morgan, 1983). It is segmented by several N70°E trending fracture zones of Pan-African age (e.g. the Adamawa also called Central Africa Shear Zone and the Sanaga Faults; Fig. 1.2). The CVL has been continuously active for the past 65 Ma and shows no age progression of volcanic activity (Fitton & Dunlop, 1985). This would suggest that the CVL cannot be interpreted as the surface expression of a single hot spot (Moreau et al., 1987; Deruelle et al., 2007; Meyer et al., 1998; Montigny et al., 2004).

The geology and petrology of the CVL have been presented by many authors such as: Geze (1943), Fitton & Dunlop (1985), Deruelle et al. (1987, 2007), Moreau et al. (1987). Mafic lavas mostly composed of alkali basalts are present in all volcanic centres (Fitton & Dunlop, 1985; Deruelle et al., 1991; Pipper & Richardson, 1972) except for Mount Etinde which is entirely composed of nephelinite (Nkoumbou et al., 1995). The oldest volcanic rock is aged 15-35 Ma from the oceanic sector (Fitton & Dunlop, 1985), and between 9 Ma (Mt. Cameroon) and 34 Ma (Mandara Mountains) from the continental sector (Tabod et al., 1992).

The oceanic segment consists of six Tertiary to Recent major volcanoes found on four islands: one each on Pagalu (former Annobon), São Tomé and Principe islands and three (Santa Isabel, Biao and San Carlos) on Bioko island formerly called Fernando Poo (Deruelle et al., 2007; Tabod et al., 1992). Pagalu Island lies directly on the oceanic crust (Moreau et al., 1987), Säo Tomé rests on Cretaceous sandstones (Tabod et al., 1992, Pipper and Richardson, 1972) and Bioko is built on the Cretaceous sedimentary basins of Douala-Rio del Rey (Deruelle et al., 1987).

The continental sector includes Etinde, Cameroon, Manengouba, Bamboutos, oku and Mandara Mounts as well as the volcanic province of Biu and Adamawa plateau (Tabod et al., 1992; Fig. 1.2). The basement is formed of Precambrian metamorphic rocks (schists and gneisses intruded by granites) covered by Cretaceous to Quaternary sedimentary rocks (mostly sandstones and small amount of limestone) upon which lavas of Mt Cameroon, the Manengouba volcano and Bambouto and Oku Mounts rest (Deruelle, et al., 1987; Deruelle et al., 1991; Tabod et al., 1992).

The continental sector of the CVL is also dotted with numerous crater lakes (formed when rising magma interact explosively with water close to the surface; Fig.1.2): lakes Nyos (1100 m a.s.l.), Monoun (1080 m a.s.l.), Barombi Koto (1400 m a.s.l.), Barombi Mbo (301 m a.s.l.) and Debundscha (65 m a.s.l.; Ngwa et al., 2010). Some of these craters have exhibited catastrophic outgassing in the past decades. For example, lakes Manoun and Nyos released carbon dioxide gas causing the death of about 37 people and more than 1700 people in 1984 and 1986 respectively (Tabod et al., 1992). The mantle-derived CO_2 trapped in these lakes is likely to have been released by limnic overturn (eruption of dissolved $CO_2$from a deep lake water; Ambey, 1989).

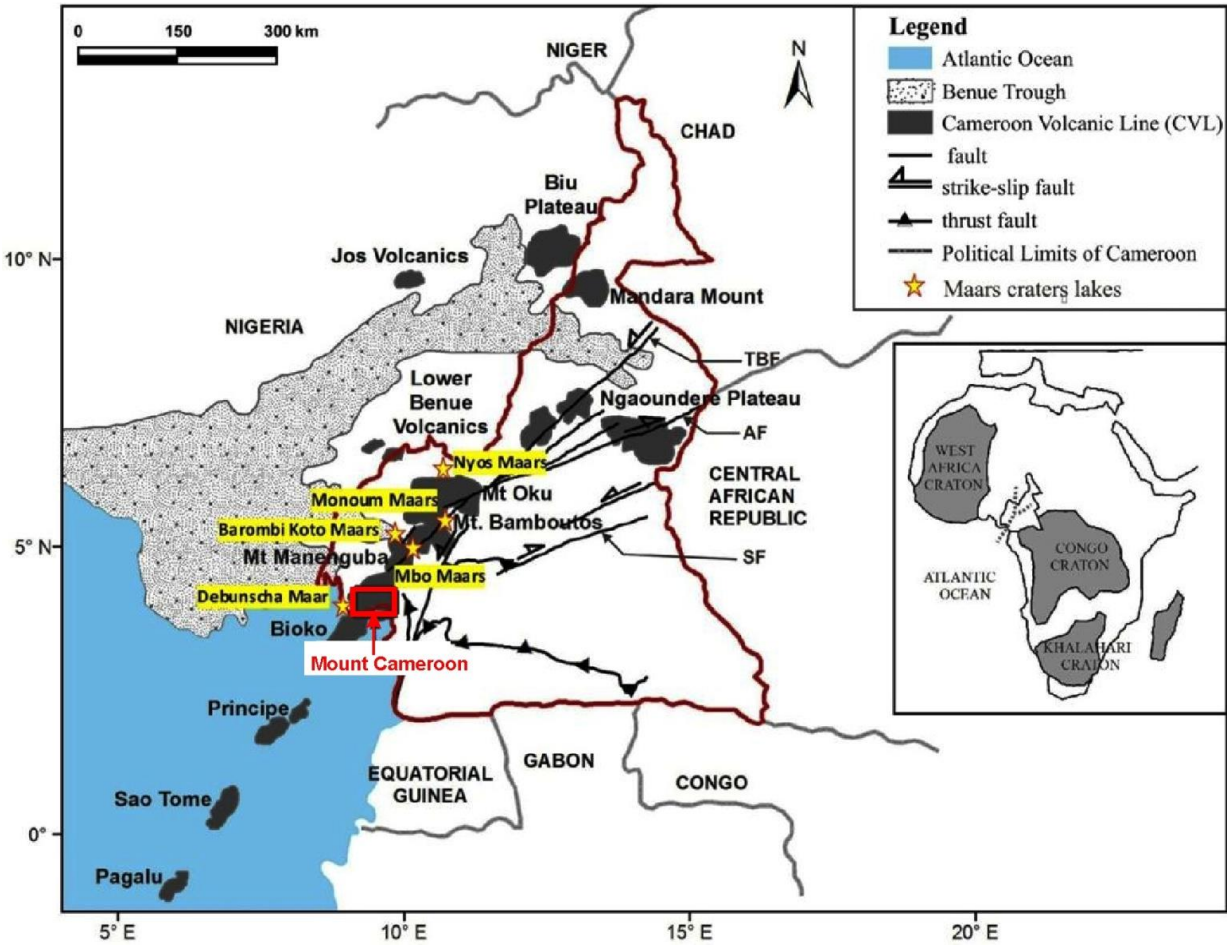

Figure 1.2 Sketch map of Cameroon showing Mount Cameroon (red rectangle), the Cameroon Volcanic Line, and the different main faults. AF, Adamaoua fault; KFC, Kribi-Campo fault; SF, Sanaga fault; TBF, Tchollire-Banyo fault (Compiled from Toteu et al., 2001; Suh et al., 2011).

The origin of the Cameroon Volcanic Line is still a controversial subject. Morgan (1983) proposes that the CVL is an expression of the weakening of the lithosphere caused by the movement of the African Plate over a hotspot during the Brasil-West Africa split. The lack of evidence of a systematic age progression of volcanism along the line expected in the case of a plume (Deruelle et al., 2007; Fitton, 1980; Fitton & Dunlop, 1985) and the presence of a deep hot zone overlain by a cold shallow one led Montigny et al. (2004) to consider the CVL as a hot line origin instead of a single hotspot. The development of a hot line is followed by crustal uplift in both the oceanic and the continental sectors. The hot line hypothesis is supported by deep-imaging seismic and gravity data of the offshore part of the CVL (Meyer et al., 1998).

The similarity in Y-shape of the CVL and the Benue trough in Nigeria has led Fitton (1980; 1983) to propose that the Cameroon Line derives from the sudden displacement at about 85 to 65 Ma of an asthenospheric hotspot beneath the Benue trough during the Cretaceous to its present

position (i.e. beneath Mt. Cameroon and the Gulf of Guinea) as a result of the major reorganisation of the African continental plates boundaries. However, the fact that no structural or geochemical data have been presented to prove this hypothesis (Deruelle et al., 1991) and the absence of magmatic activity within the Benue trough (Benkhelil, 1989) make this suggestion difficult to accept.

The continental part of the CVL coincides with the N 70°E trending faults of the Foumban Shear Zone which crosses the N 70°E trending Adamawa uplift in the north-eastern part of the line and is considered to be the continuation of the Pernambuco lineament in Brazil prior the continental separation (Toteu et al., 2001). During the opening of the Central Atlantic Ocean in Cretaceous times, the upwelling of melted material caused by the lithospheric uplift might have provoked the re-activation of the Adamawa fault zone which produced the Cameroon line volcanism (Moreau et al., 1987). Even though this model does not explain the cause of the partial melting in the mantle, it is based on structural analyses and is the most accepted hypothesis on the origin of the CVL (Deruelle et al., 2007).

Whatever may have caused the volcanism of the Cameroon line, basaltic lava that erupted from the oceanic and the continental segments are geochemically and isotopically identical providing evidence that both segments have a common mantle source origin most probably the upper mantle (Fitton and Dunlop, 1985; Fitton, 1987; Der-Chuen Lee et al., 1994). Geological and geophysical data presently available are still not enough to clearly explain the origin of the CVL.

Chapter 2

The theory of seismic and volcanic hazard assessment of a volcano

Seismic hazard assessment is the quantification of the ground-motion of a strong earthquake expected to occur at a particular site (Gupta, 2002). It can be done in two basics methods: the deterministic and probabilistic, though the probabilistic approach is much widely used (Gupta, 2011). The deterministic approach evaluates the maximum expected ground motion at a site resulting from the strongest potential earthquake (Gupta, 2002). The probabilistic method quantifies the probability that a specified level of ground motion will be exceeded at least once at a site during a specific exposure time (Gupta, 2011).

2.1 Determination of seismic hazard parameters of a selected area

The main objective of the probabilistic seismic hazard assessment (PSHA) is to quantify the probability of exceeding various ground motion level at a site, given all possible earthquake scenario (Gupta, 2002). This approach allows the integration of uncertainties in the size, location, and rate of recurrence of earthquakes and is therefore able to estimate ground motion parameter with a specified level of confidence. PSHA is essentially carried out in four steps: identification of the seismic source zones of the site of interest, determination of the seismic hazard parameters for each seismic zone, calculation of ground motion prediction and their uncertainties, and integration of uncertainties contributed by each zone (Gupta, 2011).

Each seismic source is characterised by four seismic parameters: the level of completeness m_{min}, the maximum earthquake magnitude m_{max}, the mean seismic activity rate λ and the Gutenberg-Richter parameter b. It is assumed that earthquake occurrence in time is random and follows a Poisson process such that earthquakes occur independently of each other. This implies that the occurrence of future events are not related to the occurrence of past ones and earthquake magnitudes follow a doubly truncated Gutenberg-Richter frequency-magnitude distribution (Gutenberg & Richter, 1944, 1954)

$$Log_{10}N = a - bM \tag{2.1}$$

where N is the number of events with magnitude greater than or equal to M; a is the parameter that measure the level of seismicity while b (b-value) quantifies the slope of the frequency-magnitude distribution (FMD) and describes the ratio between the number of small and large events. This relationship is of critical importance in seismology since it describes both tectonic and induced seismicity, can be applied at different time scales, and is valid over a large interval of earthquake magnitudes (Kijko & Smit, 2012). Assessment of the above parameters requires a

seismic event catalogue containing origin times, size of seismic events (in terms of magnitude or intensity) and spatial location (Kijko & Graham, 1998). It is further assumed that the magnitude M lies within the range $< m_{min}, m_{max} >$ where m_{min} represents the level of completeness of the earthquake catalogue and m_{max} is the maximum possible seismic event magnitude of a given area.

2.1.1 Estimation of the level of completeness (m_{min}) of an earthquake catalogue

The magnitude m_{min} is the minimum (threshold) magnitude above which all earthquakes of a catalogue are accurately detected (Kijko & Graham, 1999). Errors in the estimation of the level of completeness lead to under sampling if too high due to unnecessarily discarding usable data, or to spurious observations in *a*- and *b*-values if too low (e.g. Habermann, 1987).

Most methods used to estimate the level of completeness of earthquake catalogues are based on two fundamentally different assumptions (Woessner and Wiemer, 2005). Some methods are mainly built on the information provided by seismic catalogues .and assume that earthquake magnitude distribution satisfy a model of earthquake occurrence, such as a Poissonian distribution and the frequency-magnitude Gutenberg-Richter relation. In this case, m_{min} is defined as the minimum magnitude at which the cumulative frequency-magnitude distribution (FMD) departs from the exponential decay (Ambey, 1989; Fig. 2.1). Examples of procedure belonging to this category were developed by Wiemer and Wyss (2000), Woessner and Wiemer (2005), Wiemer and Katsumata (1999) amongst others. Despite the fact most methods widely used rely on this assumption, it has some weak points. For instance, levels of completeness m_{min} of the analysed catalogues estimated through this assumption solely represent the average values over space and time (Gupta, 2011).

The second assumption used for the estimation of m_{min} is based on information provided by the seismic stations recording the seismic events such as the detection capability and the signal-to noise ratio. Examples of developed techniques that follow this assumption have been proposed by Sereno and Bratt (1989), and Schorlemmer and Woesser (2008). These methods form a category of waveform-based methods and are generally not suitable to determine m_{min} (Wiemer and Wyss, 2000).

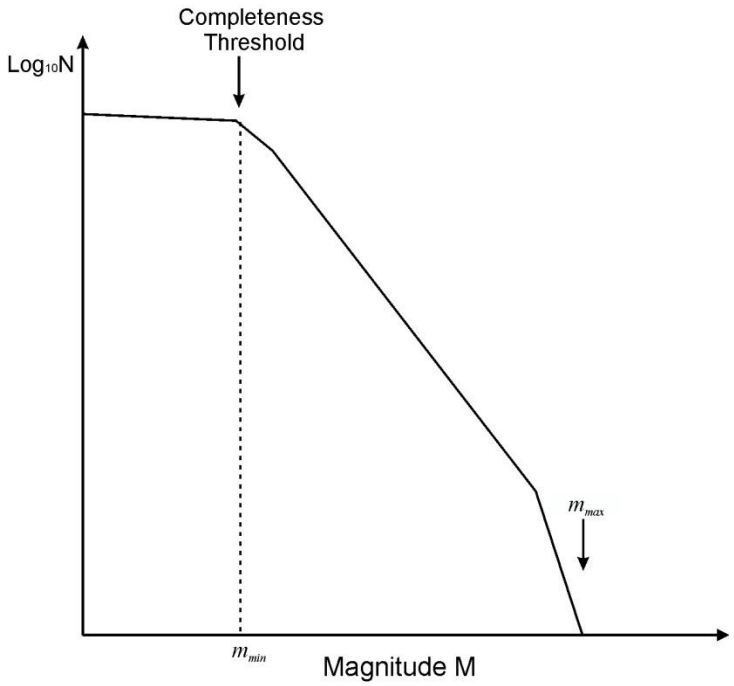

Figure 2.1: Idealised cumulative frequency-magnitude plot. N is the cumulative number of events of magnitude greater than or equal to M. m_{max} is the maximum possible earthquake magnitude and m_{nin} is the magnitude corresponding to the completeness threshold The discrepancy (flattening of the curve) at low magnitude is attributed to the incomplete detection (Ambey, 1989).

Occasionally, m_{min} is determined estimated using the day-to- night ratio of earthquake frequency by assuming that the detection threshold due to noise decreases at night (Rydelek and Sacks, 1989). However, this method is only efficient if all non-random features (e.g. swarms, aftershock sequences, mine blasts) are removed from the earthquake catalogues, thus the limitation on the applicability.

2.1.2 Estimation of the seismic activity rate λ and *b*-value of Gutenberg-Richter for time varying seismicity

The mean activity rate λ refers to the number of annual earthquakes with magnitudes equal or above m_{min} (Gupta, 2011). It is considered that earthquake occurrence over time in the given area is independent and satisfies a Poisson distribution. The variation of the *b*-value of the Gutenberg-Richter relationship is directly related to the shear stress conditions, the thermal gradient and the heterogeneity of the seismic medium with typical values ranging from 0.6 to 1.4 (Gibowicz and Kijko, 1994).

In particular, values less than 1 refer to an area of crustal homogeneity and high stress and values greater than 1 indicate crustal heterogeneity and low stress (Gridges & Gao, 2006). A notable variation of the *b*-value is observed in volcanic areas where it can be as high as 3.0, indicating that the active magmatic system can be exceptionally rich in very small earthquakes (McNutt, 2005).

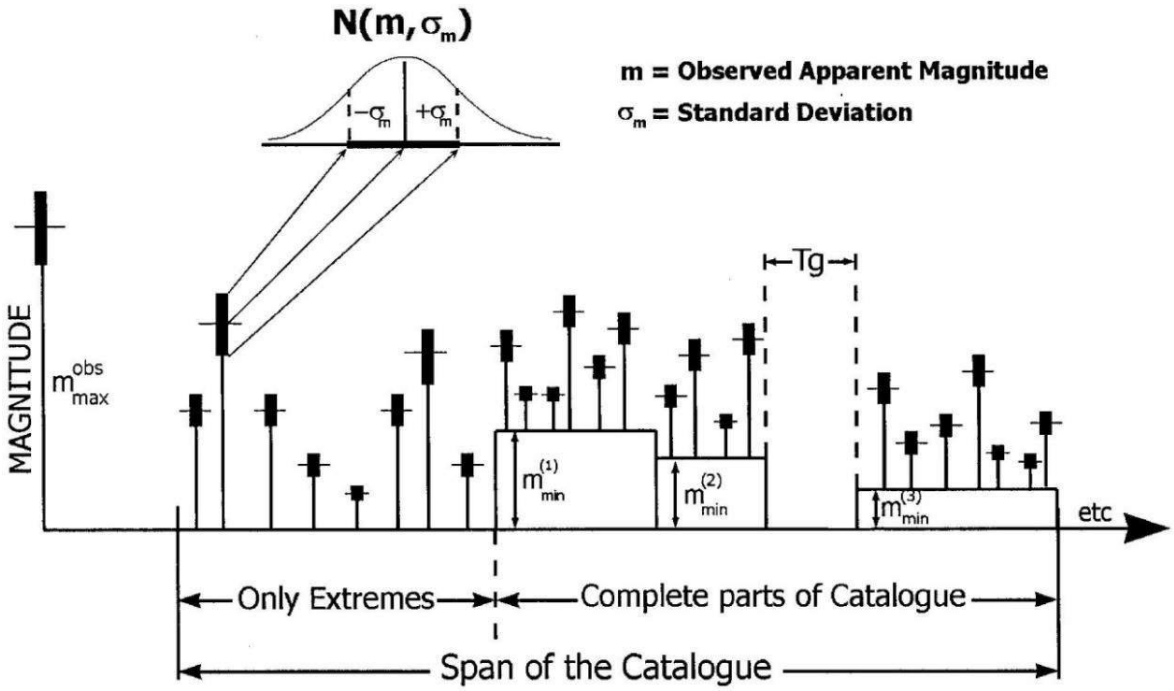

Figure 2.2: Illustration of data which can be used to obtain the maximum likelihood estimators of parameters λ and b-value; the largest historical (extreme part of the catalogue) earthquake magnitude ($\boldsymbol{m_{max}^{obs}}$) can be combined with the several complete instrumental catalogues (Kijko and Sevelloll, 1989).

Numerous challenges such as the incompleteness of the dataset and the uncertainties in magnitude determination are encountered when compiling earthquake catalogues. Historical (macroseismic) events often contain inaccuracies and misinterpretations of damages when attributing numerical values of magnitude to an earthquake. The instrumental period might also have errors either due to the incompleteness of the catalogues or the unification of the magnitude scale. All these factors need to be taken into account in the evaluation of λ and *b*. To encounter all these challenges, Kijko & Sellevoll (1989, 1992) introduced another approach that permits the utilisation of incomplete earthquakes catalogues It is assumed that a classic earthquake catalogue contains two types of information: macroseismic events that occurred over a period of few hundred years and recent instrumental data. Macroseismic events are usually the strongest events and constitute the extreme part of the data and are called the historical catalogue. The recent

instrumental data can be divided into several sub-catalogues, each assumed completed above a specified threshold of magnitude (Fig. 2.2). The method accepts gaps (no seismic events), either due to the lack of records or the non-functioning of seismic networks.

The approach commonly utilised to approximate λ and b-value parameters is the maximum likelihood (McGuire, 2004; Kijko and Sellevoll, 1989, 1992; Kijko and Smit, 2012). Let us assumed that the instrumental data can be divided into n_x sub-catalogues, each of them with a time span T_i and complete from the known magnitude $m_{min}^{(i)}$. For each sub-catalogue i, m_{ij} is the apparent magnitude, $m_{ij} \geq m_{min}^{(i)}$, $j = 1,\ldots,n_i$, where n_i is the number of earthquakes in each complete sub-catalogue and $i = 1,\ldots, n_x$.

If the size of seismic events is independent of their number, the likelihood function of earthquake magnitude in each sub-catalogue i, is the product of the likelihood functions of β (with $\beta = b \ln 10$) and λ (Kijko & Graham, 1999).

$$L_i(\lambda, \beta) = L_i(\beta).L_i(\lambda) \tag{2.2}$$

The assumption that the number of earthquakes per unit time is a Poisson random variable gives a form of $L_i(\lambda)$ equal to

$$L_i(\lambda) = \text{const}(\tilde{\lambda}_i t_i)^{n_i} \exp\left(-\tilde{\lambda}_i t_i\right) \tag{2.3}$$

where const is a normalizing factor and $\tilde{\lambda}_i$ is the apparent mean activity rate for the complete sub-catalogue i. The relation between the apparent activity rate $\tilde{\lambda}_i$ and the "true" activity rate λ_i is given by:

$$\tilde{\lambda}_i = \lambda_i C_\delta(m, \delta) \tag{2.4}$$

Where $C_\delta(m, \delta)$ is the correction function and $m_{min} \leq m \leq m_{max}$

The joint likelihood function of all the data in the catalogue, extreme and complete, is given by:

$$L(\lambda, \beta) = \prod_{i=0}^{n_s} L_i(\lambda, \beta) \tag{2.5}$$

To obtain the maximum likelihood of the parameters $\hat{\lambda}$ and $\hat{\beta}$, we have to solve by iteration the set of equations $\partial \ln L(\lambda, \beta)/\partial\lambda = 0$ and $\partial \ln L(\lambda, \beta)/\partial\beta = 0$ (Kijko & Sellevoll, 1989). For special cases where the extreme magnitudes are not taken into consideration and the catalogue is composed of only one complete part, the maximum likelihood estimators of λ and β are respectively given by:

$$\lambda = \frac{n}{T} \tag{2.6}$$

$$\frac{1}{\beta} = \bar{m} - \frac{m_{max}\exp[-\beta(m_{max})] - m_{min}\exp[-\beta(m_{min})]}{\exp[-\beta(m_{max})] - \exp[-\beta(m_{min})]} \tag{2.7}$$

where n is the number of events that occurred within the time interval T, $\beta = b\ln 10$ and $\bar{m} = \sum_{i=0}^{n} m_i / n$ is the mean magnitude of the catalogue under investigation ($\geq m_{min}$ the level of completeness). It should be noted that equation (2.7) takes the form of Page's (1968) formula for the$ maximum likelihood evaluation of β.

Additionally, if it is assumed that $m_{max} \to \infty$, equation (2.7) replaces the well-known Aki (1965) and Utsu (1965) formula classic estimator

$$\frac{1}{\hat{\beta}} = \bar{m} - m_{min} \tag{2.8}$$

It follows that for sufficiently large n, $\hat{\beta}$ is approximately normally distributed about its mean value equal to equation (2.7) with the standard deviation equal to (Gibowicz & Kijko, 1994)

$$\hat{\sigma}_{\beta} = -\left(\frac{\partial^2 \ln L}{\partial \beta^2}\right) = \hat{\beta}/\sqrt{N} \tag{2.9}$$

The standard deviation of $\hat{b}$ is obtained by dividing $\hat{\sigma}_{\beta}$ by ln(10).

2.1.3 Inclusion of *a priori b*-value information (b_{prior})

Due to the fact that seismic event catalogues are often incomplete, the knowledge of any additional information (seismogenic zones or independent geophysical or geological sources) on a parameter is crucial. As a result, the approximate value of the Gutenberg-Richter parameter b_{prior} and its standard deviation σ_{prior} are assumed to be known from historic events or taken base on another area with similar seismogenic features.

The most efficient way to include *a priori* information is to apply the formalism of the Bayesian estimation from which the value of β_{prior} can be written (Kijko & Graham, 1999)

$$\beta_{\text{prior}} = \beta + \delta\beta \tag{2.10}$$

where β is the unknown 'true' value of the parameter β and $\delta\beta$ is the unknown error on the parameter β. In cases where no information leading to the choice of the type of distribution of $\delta\beta$ is available, it is assumed that the errors $\delta\beta$ are Gaussian, with mean equal to zero and known standard deviation σ_{prior}.

2.1.4 Estimation of the area –characteristic maximum possible magnitude (m_{max})

The maximum magnitude is important in earthquake hazard estimation, particularly when assessing long return periods. Sometimes used synonymously with maximum credible earthquake, the maximum magnitude is the magnitude of the largest possible earthquake for a given seismic source such as a fault (EERI Committee, 1984). In other words, the maximum magnitude is the sharp cut-off magnitude that cannot be exceeded by any seismic event and represents the maximum strain crustal rocks are able to support (Richter, 1958). It can be estimated using a combination of factors like seismicity, geological, geophysical and structure information of the seismic source (Wheeler, 2009). Presently, there is no universally accepted procedure for evaluating the value of m_{max} but the available methodologies are generally classified into two categories, i.e. deterministic and probabilistic methods.

The deterministic approach commonly applied is based on empirical formulas that depend on the geology of seismic regions and fault parameters (i.e. fault length, rupture dimension). The information regarding the length and the different types of faults can be simulated on a computer (Ward, 1997), while the geological information is used to delineate tectonic features which control the value of m_{max} (Wheeler, 2009). In most cases, unfortunately, the value of m_{max} calculated from deterministic methods are often inaccurate and the uncertainties can reach up to one unit on the Richter scale (Kijko and Graham, 1998), i.e. $\approx 10^2$ ergs difference in terms of energy release (Richter, 1935).

When using probabilistic procedures, the value of m_{max} is estimated purely on the basis of the seismological history of the area. The choice of the suitable technique for a particular situation depends on the information available about the past seismicity and/or the assumptions about the statistical distribution model. Probabilistic techniques can be organised in three groups: parametric estimators, non-parametric estimators and fit of the cumulative density function (CDF). A detailed review of most of the available procedures is described by Kijko & Singh (2011). In this report, three parametric estimators are presented.

In general, the estimated m_{max} value is given by Kijko & Singh (2011):

$$m_{max}^{obs} + \Delta \tag{2.11}$$

where Δ is a positive correction factor and m_{max}^{obs} is the largest observed magnitude in the catalogue.

The first estimator of m_{max} is based on the formalism derived by Cooke (1979)

$$\widehat{m}_{max} = m_{max}^{obs} + \int_{m_{min}}^{m_{max}} [F_M(m)]^n \, dm \tag{2.12}$$

where $F_M(m)$ is the cumulative density function (CDF) of a random variable m. For the frequency magnitude Gutenberg-Richter relation in equation (2.1), the respective CDF becomes (Page, 1968):

$$F_M(m) \begin{cases} 0, & \text{for } m < m_{min} \\ \dfrac{1 - \exp[-\beta(m - m_{min})]}{1 - \exp[-\beta(m_{max} - m_{min})]}, & \text{for } m_{min} \le m \le m_{max} \\ 1, & \text{for } m > m_{max} \end{cases} \tag{2.13}$$

Following equation (2.11), the maximum regional earthquake magnitude m_{max} is equal to the largest observed magnitude m_{max}^{obs}, added by an amount $\Delta = \int_{m_{min}}^{m_{max}} [F_M(m)]^n \mathrm{d}m$. Based on equation (2.12), the estimator of m_{max} requires the calculation of the integral

$$\Delta = \int_{m_{min}}^{m_{max}} \left[\frac{1 - \exp[-\beta(m - m_{min})]}{1 - \exp[-\beta(m_{max} - m_{min})]}\right]^n \mathrm{d}m \tag{2.14}$$

This equation does not have a simple solution but, can be estimated through the application of Cramér's approximation. According to Cramér (1961), for large n, the value of $[F_M(m)]^n$ is approximately equal to $\exp\{-n[1 - F_M(m)]\}$. After the replacement of $F_M(m)]^n$ by its Cramér's approximation followed by some calculations, the integral (2.14) becomes

$$\Delta = \frac{E_1(n_2) - E_1(n_1)}{\beta \exp(-n_2)} + m_{min} \exp(-n) \tag{2.15}$$

Where $\beta = b \ln 10$ $n_1 = n/\{1 - \exp[-\beta(m_{max} - m_{min})]\}$,$n_2 = n_1 \exp[-\beta(m_{max} - m_{min})]$, and $E_1(.)$ denote an exponential integral function. Hence following equation (2.12), for the Gutenberg-Richter frequency-magnitude relation, the estimator of m_{max} is obtained as an iterative solution of the equation

$$m_{max} = m_{max}^{obs} + \frac{E_1(n_2) - E_1(n_1)}{\beta \exp(-n_2)} + m_{min} \exp(-n) \tag{2.16}$$

Kijko & Sellevoll (1989) introduced equation (2.16) and the solution is termed the Kijko-Sellevoll (in short K-S) estimator of maximum magnitude. In this case, the variance is given by (Kijko, 2004):

$$\mathrm{VAR}(\hat{m}_{max}) = \sigma_M^2 + \left[\frac{E_1(n_2) - E_1(n_1)}{\beta \exp(-n_2)} + m_{min}\exp(-n)\right]^2 \qquad (2.17)$$

where σ_M represents the epistemic variability which is the uncertainty produced by the application of the wrong mathematical model in the process (e.g.: an inadequate CDF) or incorrect value of the model parameters (e.g.: *b*-value). The second part of the variance represents the aleatory variability of m_{max}, i.e. the one inherent in the randomness of the earthquake generation process. The solution of equation (2.17) quantifies the uncertainty of maximum magnitude determination.

where σ_M is the standard error in the determination of the largest observed magnitude m_{max}^{obs} . This procedure based on the Cramér's approximation provides a better estimator of m_{max} compare to the T-P estimator (Kijko & Graham, 1998). Since the above procedure is based on the Cramér's approximation, it gives a correct estimation of m_{max} only for large number of earthquakes.

However, the second estimator is an alternative approach, correct for any number of observations and, based on the 'exact solution' of equation (2.16). If *n* is a positive integer, the integral (2.14) can be expressed as (Dwight, 1961)

$$\Delta = \frac{m_{max} - m_{min} + \frac{1}{\beta}\sum_{i=1}^{n}\frac{(-1)^i}{i}\binom{n}{i}(1 - \exp[-i\beta(m_{max} - m_{min})])}{(1 - \exp[-\beta(m_{max} - m_{min})])} \qquad (2.18)$$

It follows from equations (2.12) and (2.14) that the exact estimator of m_{max} is obtained from the following equation

$$\hat{m}_{max} = m_{max}^{obs} + \frac{(m_{max} - m_{min}) + \sum_{i=1}^{n}\frac{(-1)^i}{i}\binom{n}{i}(1 - \exp[-i\beta(m_{max} - m_{min})])}{(1 - \exp[-\beta(m_{max} - m_{min})])} \qquad (2.19)$$

The solution of equation (2.19) is called Kijko-Sellevoll (K-S) exact solution and gives the estimator of m_{max} when the earthquake magnitude distribution follows the Gutenberg-Richter relation. The approximated variance is of the form

$$\mathrm{VAR}(\hat{m}_{max})$$
$$= \sigma_{\mathrm{M}}^2 + \left[\frac{(m_{max} - m_{min}) + \frac{1}{\beta}\sum_{i=1}^{n}\frac{(-1)^i}{i}\binom{n}{i}(1 - \exp[-\mathrm{i}\beta(m_{max} - m_{min})])}{(1 - \exp[-\beta(m_{max} - m_{min})])}\right]^2 \qquad (2.20)$$

where σ_M denotes the standard error in the determination of the largest observed magnitude m_{max}^{obs} .

Estimators of m_{max} derived from the above procedures suppose that: (1) the seismic activity remains constant in time, (2) the occurrence of earthquakes in time follows a Poissonian distribution and (3) the parameters of the assumed distributions functions (λ, b-value, m_{min}) are known without errors.

Any seismogenic process can be composed of temporal trends, cycles, oscillations and pure random fluctuations. Thus, alternative techniques that incorporate various supporting data (geological, geophysical, palaeoseismicity and tectonic information) have been introduced (Cornell, 1994; Kijko & Singh, 2011; Kijko, 2004). In fact, when the variation of seismic activity is a random process, the formalism in which the model parameters are treated as random variables is a powerful tool to include uncertainties overlooked in the previous estimators' techniques.

The third parametric estimator of m_{max} is based on the formalism of Bayes. This method takes into account the uncertainty of the Gutenberg-Richter parameter b. In such case, the variation of the β-value ($\beta = b \ln 10$) in the frequency-magnitude Gutenberg-Richter relation may be represent by a Gamma function with parameters p and q. The Bayesian CDF of earthquakes magnitude takes the form (Campbell, 1982):

$$F_M(m) = \begin{cases} 0 & \text{for } m < m_{min,} \\ C_\beta \left[1 - \left(\dfrac{p}{p + m - m_{min}}\right)^q\right] & \text{for } m_{min} \le m \le m_{max,} \\ 1, & \text{for } m > m_{max,} \end{cases} \qquad (2.21)$$

where C_β is a normalizing coefficient known as the Bayesian exponential-gamma CDF of earthquake magnitude and equal to $\{1 - [p/(p + m_{max} - m_{min})]^q\}^{-1}$, $p = \bar{\beta}/(\sigma_\beta)^2$ and $q = (\bar{\beta}/\sigma_\beta)^2$. The symbol $\bar{\beta}$ denotes the known mean value of the parameter β and $\sigma_\beta$is the standard deviation of β.

The knowledge of the equation (2.21) enables to establish the Bayesian version of the estimator of $m_{max.}$ Following equation (2.12), the estimator of m_{max} requires the calculation of the integral

$$\Delta = (C_\beta)^n \int_{m_{min}}^{m_{max}} \left[1 - \left(\frac{p}{p + m - m_{min}}\right)^q\right]^n \mathrm{d}m \qquad (2.22)$$

which, after application of Cramér's approximation (Cramér, 1961), can be expressed as

$$\Delta = \frac{\delta^{(\frac{1}{q}+2)} \exp[\frac{nr^q}{1 - r^q}]}{\beta} \left[\Gamma\left(-\frac{1}{q}, \delta r^q\right) - \left(-\frac{1}{q}, \delta\right)\right] \qquad (2.23)$$

where $r = p/(p + m_{max} - m_{min})$, $\delta = nC_{\beta}$, and $\Gamma(.,.)$ is the complementary Incomplete Gamma Function. The estimator of m_{max}, when the uncertainty of the b-value is taken into consideration, is calculated as an iterative solution of the equation (Kijko, 2004)

$$m_{max} = m_{max}^{obs} + \frac{\delta^{(\frac{1}{q}+2)}\exp[nr^q/(1-r^q)]}{\beta}\left[\Gamma\left(-\frac{1}{q}, \delta r^q\right) - \left(-\frac{1}{q}, \delta\right)\right] \qquad (2.24)$$

The value of m_{max} obtained from the solution of equation (2.24) will be denoted as the Kijko-Sellevoll-Bayes estimator of $m_{max,}$ or in short K-S-B.

The approximate variance of the K-S-B estimator of m_{max} for the frequency-magnitude Gutenberg-Richter distribution is of the form (Kijko & Singh, 2011):

$$\mathrm{VAR}(\hat{m}_{max}) = {\sigma_M}^2 + \left[\frac{\delta^{(\frac{1}{q}+2)}\exp[nr^q/(1-r^q)]}{\beta}\left[\Gamma\left(-\frac{1}{q}, \delta r^q\right) - \left(-\frac{1}{q}, \delta\right)\right]\right]^2 \qquad (2.25)$$

The assessment of the seismic parameters requires a seismic event catalogue containing origin times, event magnitudes and the spatial location of earthquakes so that the PDF can be calculated (Gupta, 2011).

In an assessment of volcanic hazard, it is vital to consider the probability of a future eruption. Statistical modelling using eruption records have been applied to various volcanoes to predict the spatial patterns, the frequencies, and the probabilities of eruptions for risks assessment (Wickman, 1966; Ho et al., 1991; Jones et al., 1999; Caniaux, 2005) Eruptions usually occur in a random process and a Poisson distribution provides a suitable model for such behaviour.

2.2 Statistical analysis of a volcano

Applications of statistical methods to volcanic eruptions began with the research of Wickman (1966, 1976) who discussed various Poisson models applied to a number of volcanoes with different styles of activity. He observed that the eruption recurrence rates of those volcanoes are not time dependent and can be termed 'Simple Poissonian Volcanoes'. The Poisson distribution is an excellent distribution for rare events such as the case of volcanic events.

When applying a Poisson model, it is assumed that volcanic eruptions occur randomly, i.e. eruptions occur independently of each other. In a Poisson distribution, if X denotes 'the number of eruption per unit time', then the probability of $X = x$ is given by (Haight, 1967):

$$P(X = x) = \frac{e^{-\lambda}\lambda^x}{x!} \qquad \text{for } x = 0,1,2,\ldots \qquad (2.26)$$

where λ is the rate of occurrence of volcanic eruptions and is assumed to remain constant throughout the time. In a Poisson process, if eruption events happen at a mean rate λ per unit of time, then the total number of occurrences during an interval of time t is λt. Also, the time between two eruptions follows an exponential distribution whose PDF is given by (Haight, 1967)

$$f(t) = \lambda e^{-\lambda t} \tag{2.27}$$

The rate of occurrence λ is also known as the intensity function of distribution. Since the work of Wickman (1966), this probability law has been applied in various types of volcanoes, from basaltic (Klein, 1982) to stratovolcano (Jones et al., 1999, Caniaux, 2005). Two different methods based on the maximum likelihood estimate method and both relying on the number of events occurring over a certain period of time are used to evaluate the parameter λ.

The first one is based on Poisson count data and is proposed by Ho et al., (1991). Let assume that $x_1, x_2, \dots, x_n$ represent the observed frequency of eruption (number of eruption per unit of time) in a random sample of size *n;* the likelihood function of such Poisson distribution with parameter λ is given by:

$$L(\lambda) = \prod_{i=1}^{n} f(x_i;\lambda) = \prod_{i=1}^{n} \frac{e^{-\lambda}\lambda^{x_i}}{x_i!}$$

$$= \frac{e^{-\lambda}\lambda^{x_1}}{x_1!} \dots \frac{e^{-\lambda}\lambda^{x_n}}{x_n!} = \frac{e^{-n\lambda}\lambda^{\Sigma x_i}}{x_1! \dots x_n!}$$

$$L(\lambda) = \frac{e^{-n\lambda}\lambda^{\Sigma x_i}}{\prod_{i=1}^{n} x_i!} \tag{2.28}$$

Most statistical methods use the parameters values that 'best' explain the observed data. One way of doing that is to select a function that maximise parameters values of the given set of data (Consul, 1989). This technique is called the maximum likelihood estimation (MLE).

For computational convenience, the log-likelihood $\ln L(\lambda)$ (which also maximises λ) is alternatively used. For a random sample from a Poisson distribution, the log-likelihood function is:

$$\ln L(\lambda) = -n\lambda + (\ln\lambda)\sum_{i=1}^{n} x_i - \ln\left(\prod_{i=1}^{n} x_i!\right) \tag{2.29}$$

To find the maximum likelihood estimator $\hat{\lambda}$, we equate to zero the first partial derivative of ln$L$ with respect to λ (Consul, 1989):

$$\frac{d}{d\lambda}\ln L(\lambda) = -n + \sum_{i=1}^{n}\frac{x_i}{\lambda} = 0 \tag{2.30}$$

The solution of equation (2.30) is the maximum likelihood estimator of λ and is given by (Ho et al., 1991):

$$\hat{\lambda} = \sum_{i=1}^{n}\frac{x_i}{n} = \bar{x} \tag{2.31}$$

This shows that the annual recurrence rate $\hat{\lambda}$, is the average number of eruptions x_i during the observation period *n* (in years). The estimation of $\hat{\lambda}$ in this model does not require an individual observation of the events x_i.

The second method to estimate the eruption rate is derived according to Jones et al. (1999). Mathematically, depending on the availability of recorded eruptions, the assumptions for a Poisson distribution are as follows:

(i) *n* eruptions have occurred during a period of time *X*, but the eruptions date are not known, i.e. *n-1* consecutive events of that period are not dated. In such case, the probability is written as

$$f(t) = (1 - e^{-\lambda X})^n \tag{2.32}$$

(ii) an event occurred within a known period *Y*, i.e. two consecutives eruption events are dated, the probability is given by

$$f(t) = \lambda e^{-\lambda Y} \tag{2.33}$$

(iii) no event have occurred for a period of time *Z* since the last dated eruption, the probability is:

$$f(t) = e^{-\lambda Z} \tag{2.34}$$

λ is assumed to remain constant throughout, since this is the rate of occurrence of volcanic eruptions.

Assuming that all eruptions of a chronological series are independent from one and another, the joint probability density function *F* (likelihood function) is the product of all the probabilities

and is given by:

$$F = \prod_{i}^{I}(1 - e^{-\lambda X_i})^{n_i}\prod_{j}^{J}\lambda e^{-\lambda Y_j}.e^{-\lambda Z} \tag{2.35}$$

To determine the parameter λ, the natural logarithm of the equation is taken and differentiated with respect to λ, the resulting expression is made equal to zero and solved using an appropriate method (Jones et al., 1999).

The natural logarithm of the likelihood function is:

$$\ln F = \sum_{i}^{I} n_i \ln\left(1 - \mathrm{e}^{-\lambda X_i}\right) + \sum_{j}^{J} (\ln \lambda - \lambda Y_j) - \lambda Z \tag{2.36}$$

The partial derivative of equation (2.36) with respect to the parameter λ is given by:

$$\frac{\mathrm{d}\ln F}{\mathrm{d}\lambda} = \sum_{i}^{I} \frac{n_i X_i \mathrm{e}^{-\lambda X_i}}{1 - \mathrm{e}^{-\lambda X_i}} \sum_{j}^{J} \left(\frac{1}{\lambda} - Y_j\right) - Z$$

$$\text{Hence} \quad \frac{\mathrm{d}\ln F}{\mathrm{d}\lambda} = \sum_{i}^{I} \frac{n_i X_i}{\mathrm{e}^{\lambda X_i} - 1} \sum_{j}^{J} \left(\frac{1}{\lambda} - Y_j\right) - Z \tag{2.37}$$

The estimation of the Poisson parameter λ in event where all the volcanic eruptions dates are not known is calculated as an iterative solution of the equation:

$$\sum_{i}^{I} \frac{n_i X_i}{\mathrm{e}^{\lambda X_i} - 1} \sum_{j}^{J} \left(\frac{1}{\lambda} - Y_j\right) - Z = 0 \tag{2.38}$$

The parameters n_i, X_i, Y_j and Z are derived based on the eruption chronology of the volcano.

Note that if all the eruptions are dated, then equation (2.38) becomes:

$$\frac{J}{\lambda} = Z + \sum_{j}^{J} Y_j$$

$$\Leftrightarrow \lambda = \frac{J}{\left(Z + \sum_{j}^{J} Y_j\right)} \tag{2.39}$$

where Y the elapsed time (in years) between two consecutives dated eruptions, J is the total number of dated eruption and Z is the time (in years) since the occurrence of the last dated eruption. The advantage of this method relies on the fact that it is possible to determine λ even if all volcanic eruptions of a given volcano are not dated.

Chapter 3

Geological Setting and historical lava flow at Mount Cameroon Volcano

3.1 Morphology, local geology and structure

Mount Cameroon is an elliptical-shaped stratovolcano of ~ 4095 m above mean sea level, found midway along the volcanic center of the CVL (Suh et al., 2003; Fig 1.2). It measures 50 by 35 km at its base and contains a total volume of lava estimated at 1200 km^3 (Geze, 1953; Suh et al., 2003). The volcano has over 100 volcanic cones, explosion craters and lava flows covering both the plateau and summit regions (Geze, 1953; Fitton, 1987).

The whole massif is essentially made of basaltic lavas except his SW flanks represented by Mount Etindé which is entirely made of nephelinites. It is bounded to the NW and SE by the Rio del Rey and the Douala basins respectively (Deruelle et al., 1987; Tsafack et al., 2009). General reviews of the geology of Mt Cameroon have been provided by Geze (1953), Fitton (1987), and Deruelle et al. (1987). Figure 3.1 represents a simplified geological map of the Mount Cameroon and its surroundings.

The general geology of Mt. Cameroon is represented by a Precambrian metamorphic basement (schists and gneisses intruded by granite and diorites), covered by Cretaceous to Recent sedimentary rocks (sandstones, claystone, small amounts of shale and limestone) of the Douala and Rio del Rey basins (Ambey, 1989; Deruelle et al., 1987).

The volcanic rocks of Mt. Cameroon are essentially composed of basanites (60% in volume) and alkaline basalts (25% in volume), interbedded with small amounts of hawaiites and mugearites (Deruelle et al., 1991; Tsafack et al., 2009). Recent K- Ar dating of eight lava flows has yielded ages in the range of 2.83 Ma (Late Pliocene) to 0.00 Ma (Tsafack et al., 2009).

Only two principal normal faults have been initially mapped around the volcano: the Tiko fault (TF) to the east and the Boa fault (BF) to the west (Ambey, 1989; Fig. 3.1). However, many small fractures and crevasses are found on the plateau of the summit (SW-NE and NW-SE trends; Gèze, 1953) and the NW flank of the volcano is marked by circular steep structures (the NW cirque) and the Bokosso fault system Ateba et al., 2009; Fig 3.1). Also identified by Zogning (1988), is the Ekona fault on the east flank of the volcano (Fig. 3.1).

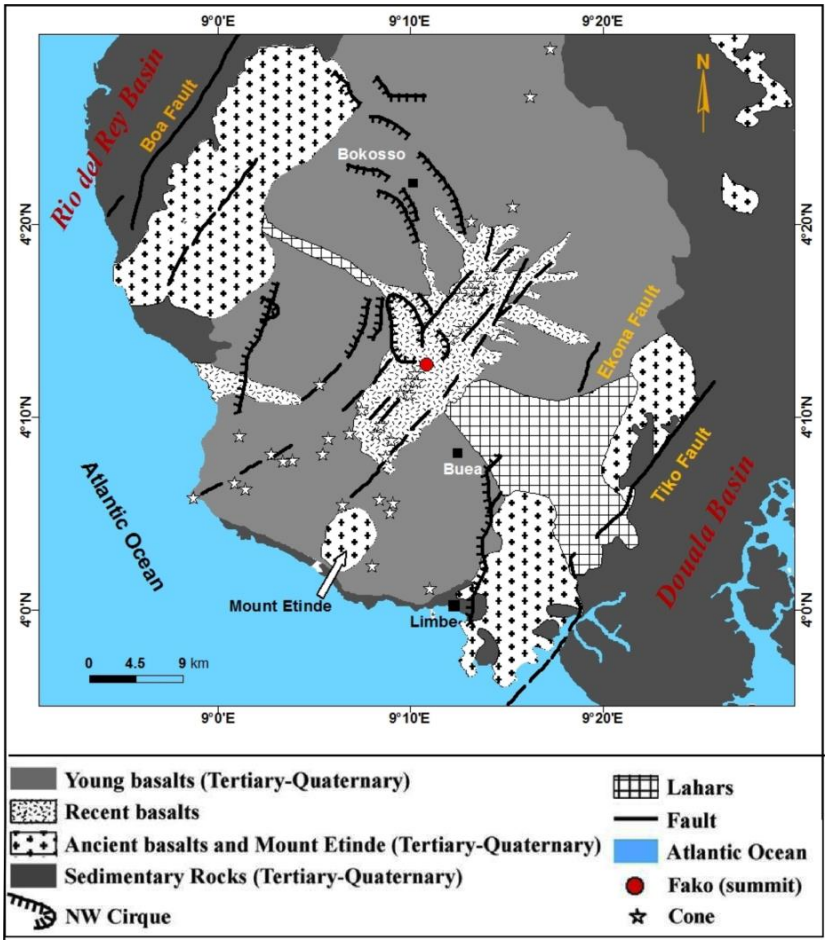

Figure 3.1 Simplified geological map of Mount Cameroon area (Ateba et al., 2009).

3.2 Geophysical observations

Information inferred from geophysical studies such as gravity and magnetic provides a better understanding of the sub-surface geology. Even though the CVL is a significant feature on the African plate, few geophysical works have been carried out and are summarised below.

3.2.1 Gravity studies

Gravity surveys have been done in Cameroon and environs by individuals, institutions and oil companies as separate small projects or regional surveys (Collignon, 1968; Okereke and Fairhead, 1984). These data, together with some aeromagnetic data, were used by Nnange et al. (2000) to examine the crustal thickness variations throughout the Adamawa plateau region (Fig. 1.1). There is a steep NE trending Bouguer gravity anomaly representing the Sanaga Fault Zone and the Foumban Shear Zone (members of the Central African Shear Zone; Fig. 1.1). The depth to the Moho was found to range between 30 km and 37 km underneath the CVL. In particular, the crustal thickness in the Adamawa plateau region varies from 18 to 23 km. It is about 35 km

in southern Cameroon and may be up to 45 km in the northern part of the Congo Craton. Beneath the Benue Trough (Fig. 1.2), the crustal thickness varies between 15 km (lower Benue) and 33 in the upper part (Poudjom et al., 1995).

3.2.2 Aeromagnetic studies

Aeromagnetic data set covering some parts of Cameroon territory were acquired in 1970 the final report of Paterson et al., *(*1976) and was accompanied by residual magnetic anomaly maps. Several workers have used those maps to enhance magnetic bodies and delineate tectonic features in Cameroon (e.g. Feumoe et al., 2012; Ndougsa et al., 2013; Bikoro et al., 2014) The southern Cameroon was affected by a series of tectonic events due to the collision between the Pan-African belt and the Congo that yielded a series of buried thrust faults (Toteu et al., 2001; Fig. 1.2). Modelling of aeromagnetic data of the central and south-east Cameroon areas depicted an abundance of lineaments that could be related to those faults and partially delineated the transition between the Congo Craton and the Pan-African domain (Feumoe et al., 2012; Ndougsa et al., 2013). These studies also highlight the fact that part of the Pan-African belt lies on top of the Congo Craton A quantitative interpretation of aeromagnetic data in the south-east Cameroon indicates the presence of iron ore formations such as magnetite and haematite with volume varying from 1.2 to 180 km^3 (Bikoro et al., 2014).

3.2.3 Seismological studies

Seismological studies have been done in the north of Cameroon (Central African Shear Zone), and along the CVL. Recordings of a quarry blast across the Adamawa plateau were utilised by Stuart et al. (1985) in a seismic refraction analysis in order to determine the crustal structure of the region. These data showed that the eastern arm of the Benue trough (Garoua Rift) is characterised by a thinned crust of ca. 23 km thickness underlain by the upper mantle with a P-wave velocity of 7.8 km/s. The crustal thickness below the Adamawa uplift abruptly varies from 23 km (thin crust) in its northern part to 33 km (normal crust) in the southern part where the P-wave velocity of the upper mantle is 8.0 km/s (Stuart et al., 1985; Plomerová et al., 1993).

Recently, 1-D shear wave velocity models were used by Tokam et al., (2010) to study the crustal structure beneath the CVL and surrounding regions in Cameroon. According to their models, in general, the crustal thickness beneath the CVL is between 35-39 km, while it is suggested to be thicker beneath the northern margin of the Congo Craton (43-48 km) and thinner under the Garoua Rift (26-31 km).

Geophysical and geological studies show that the depth to the Moho is approximately 23 km underneath the Adamawa uplift. This means that the crust is thinner than normal (~33 km) suggesting a weakening of the lithosphere below both the CVL and the Adamawa Plateau which may represent a preferred magma conduit (Poudjom et al., 1995; Plomerová et al., 1993).

3.3 Felt Earthquakes

The lack of written records makes the compilation of a complete historical seismicity data base for Cameroon very difficult. The establishment of the World Wide Standardised Seismogram Network (WWSSN) in the 1960's led to an increase in the detection of earthquakes worldwide which tremendously improved the instrumental study of the seismicity of Africa.

Ambraseys & Adams (1986) reported over 20 felt earthquakes in Cameroon for the period between 1852-1984, which formed the basis for the, so far, most completed study carried out on the seismicity of West Africa. These tremors are plotted in Fig. 3.2 together with felt events from 1984 to 2013.

Two seismicity zones are noticeable: (1) the seismicity associated with the SSW-NNE trend of the CVL and the FSZ with a predominance around Mount Cameroon; (2) the seismicity around Kribi (also trending SSW-NNE) probably connected with a fracture zone (parallel to the FSZ) and the northern margin of the Congo Craton which is still not well delimited in the southern Cameroon (Ambey, 1989; Tabod et al., 1992).

The earliest seismic event felt in Cameroon occurred in 1852 in the Mount Cameroon area where most of the felt earthquakes are associated with eruption activities of Mt. Cameroon volcano (Ambraseys & Adams, 1986). During the period 1987 to 1991, there has been an increase in seismic activity around Mt Cameroon and in the Kribi area (Tabod et al., 1991). The largest earthquake with body wave magnitude m_b = 4.8 originating near Tibati on the Foumban Shear Zone (Fig. 3.2) was recorded by Mt. Cameroon station on January 1987 (Tabod et al., 1991). In 1983, two small earthquakes of magnitude 3.9 and 4.1 at the local scale occurred near Taparé (Eastern province) and at Magba (Western province) respectively (Tabod et al., 1991). A small earthquake with an intensity magnitude of about V occurred in Garoua-Boulai in November 1986. In February and August 1986, two swarms of earthquakes were felt in the Bokosso area in the northwest province of Cameroon (Mt. Cameroon region) with a maximum intensity of V (Ubangoh, 1997). Some earthquakes with unreported intensity magnitude have also been felt in the Mt. Cameroon region (Tabod et al., 1991). For example, an earthquake was felt close to Bokosso on the north eastern flank of Mt. Cameroon (Fig 3.1) on the 29 May 1989. Also, two earthquakes were felt on the 20 and 25 September 1990 around the Buea region.

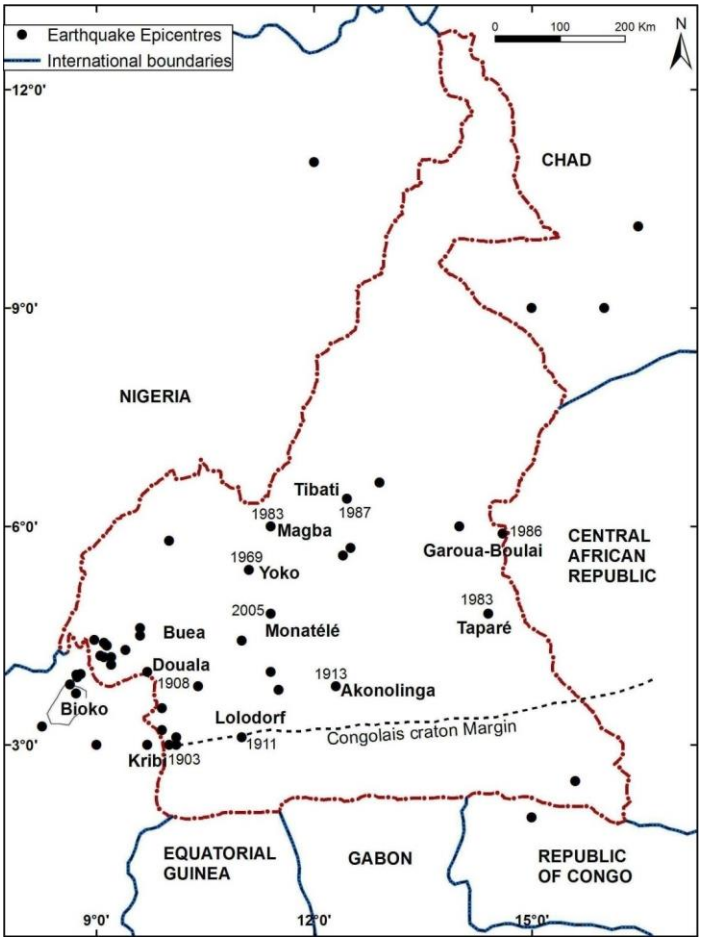

Figure 3.2: Felt Earthquakes in Cameroon and environs from 1852 to 2013 (compiled from Ambraseys and Adams, Tabod et al., 1991).

Historic seismicity shows that in 1903, the town of Kribi was shaken by an intensity V earthquake (Ambraseys and Adams, 1986; Fig. 3.2). An isoseismal map of the felt earthquake that occurred in the southern Cameroon in the last hundred years is given in Fig. 3.3. About 11 earthquakes occurred in the Kribi region between 1987 and 1989 (Ateba et al., 1992). A small earthquake of duration magnitude m_d = 2.6 was recorded by the Mt Cameroon seismic array on the 18 August 1987 Inhabitants of the kribi region have experienced five earthquakes with small damages in September 1987 with duration magnitude ranging between 2.8 and 4. Mt. Cameroon seismic array also detected two earthquakes originating from the Kribi region in 1988: on the 19 March and the 02 October with duration magnitude of 3.4 and 3.0 respectively. One year later, on March 14 and March 16 two earthquakes of duration magnitude 2.8 and 3 respectively were recorded to have originated from the Kribi area. Recently. A local magnitude of 3.04 was felt in Monatélé situated along the Sanaga Fault (Ndikum et al., 2014).

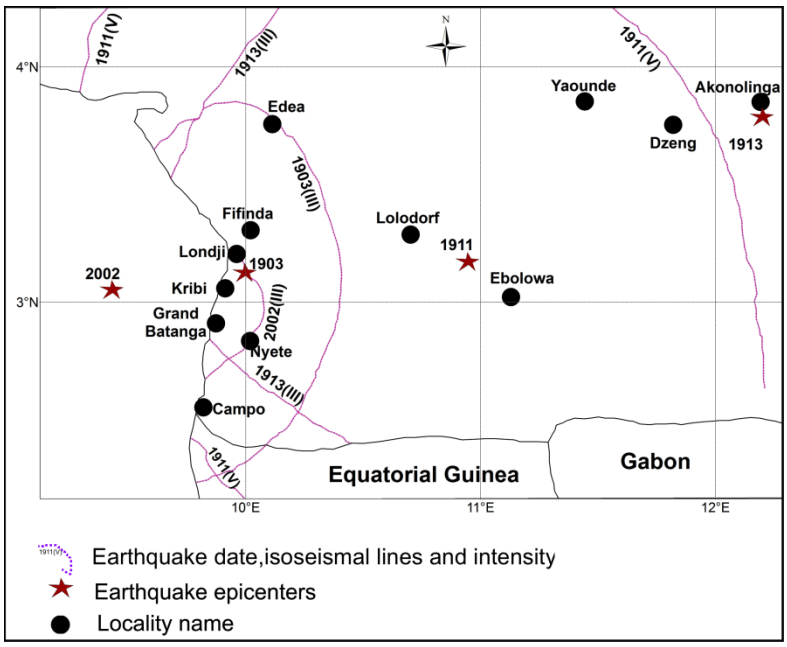

Figure 3.3: Isoseismal map of earthquakes felt in southern Cameroon within the last hundred years (Ntepe et al., 2004)

3.3 Known eruption history

According to several historians, the earliest existing record of Mount Cameroon as an active volcano comes from the narrative of Carthaginian explorer Hannon, who named it "Chariot of the God", during his journeys along the African coast around 500 BC (Gèze, 1953). Due to the presence of lava flow found by Dr. Otto Mann (Anonymous, 1910), Mount Cameroon is likely to have erupted many times in the 19th century. Guillaume (1966) and Deruelle et al. (1987) presented some information on those eruptions even though they are often vague and uncertain as to the place and date of occurrence.

3.3.1 19th century eruptions

Between 1800 and 1815, Mount Cameroon erupted at an altitude of 2600 m producing lava that reached the village of Mapanja (south-eastern flank of the mountain). Before 1835, another eruption occurred with no further information. Between 1838 and 1839, a summit eruption was recorded with no further details (Déruelle et al., 1987). In 1852, an eruption occurred on the western flank of the Mount Cameroon followed by an earthquake swarm recorded around the Bokosso–Munyenge area (Ubangoh et al., 1997). A summit eruption was furthermore recorded in 1865 and it is likely that an eruption also originated from the Mt. Cameroon volcano in January 1866 (Guillaume, 1966). Lastly, Mount Cameroon volcano erupted on its NW flank in 1868 (Déruelle et al., 1987).

3.2.2 20th and 21st century eruptions

Circa six eruptions, summarised in table 2.1, which occurred during the 20th and 21st century are well described by geologists. The earliest eruption of the 20th century on the NE flank of Mount Cameroon occurred on the 26th April 1909 (Gèze, 1953; Guillaume, 1966). This eruption was characterised by the record of long seismic swarms and earthquakes strongly felt around Buea before (1869, 1905, 1908) during (1909) and after (1910) the eruption (Ubangoh et al., 1997). In total, approximately 5 million $m^3$of lavas flowed down the slope at a speed of 4 to 5 meter per minute and large amounts of ash had fallen on the north-western side of the volcano (Anonymous, 1910; Gèze, 1943). However no damage was done since the mountain was generally surrounded by an uninhabited area (Anonymous, 1910).

In February 1922, a small eruption occurred ca. 1.5 km SW of the summit, followed by a much larger emission of lava from craters on the SW flank of the mountain (Ruxton, 1922). Many earthquakes of various intensities were felt in Buea prior these eruptions (Ubangoh et al., 1997) with some registered by seismographs in Europe (Ruxton, 1922). The lava flows reached the sea in the Bibundi area (Fig. 3.4), after destroying banana and palm oil plantations, a few houses and the main road from Limbe (formerly Victoria) to Idenau (Suh et al., 2003). The path of the 1922 lava flows can be clearly observed today thanks to the reconstruction of the road (Deruelle et al., 1987). The total volume of lava flow was estimated at 10 million m^3. They travelled at a speed of about 60-90 meters per minute (Ruxton, 1922; Guillaume, 1966).

A summit eruption in June 1954, lasting for about three weeks produced ash, explosions and minor amounts of fresh lava (De Swardt, 1956). The ejected materials mainly consisted of dark-grey to black vesicular fragments of porphyric basaltic lava.

Five years later, the 1959 eruption occurred from four craters (of which three emitted lava) at around 1500 m altitude on the eastern slope of the volcano (Jennings, 1959). The 1.5 km wide main flow destroyed several small cocoyam and banana farms before stopping just 1 km away from Ekona town (Njome et al., 2008; Fig.3.4). Many earthquakes were recorded and felt in the Buea – Limbe region during this eruption (Ubangoh et al., 1989). Unlike the previous ones, the 1959 eruption has been documented for its morphology, petrology, and geochemistry (Njome et al., 2008; Suh et al., 2008).

Table 3.1: Historical data of lava flows on Mount Cameroon since 1909

Start date (duration)	Site (s)	Elevation (m) (a.s.l)	Eruption style	Product (s)	Volume of lava flow (10^6 m^3)	Direction of the flow	Sources
26 April 1909 (unknown)	NE flank	~2390	Strombolian and Hawaiian	Lava (aa), gases, tephra	~ 5	NW slopes to Bavenda	Geze (1943), Wantim (2011)
February 1922 (~7 months with some breaks)	Summit & SW flank	~3050(1) ~1300(2)	Strombolian and Hawaiian	Lava (pahoehoe), gases, tephra	~ 10	West flank to the coast (Bibundi)	Ruxton (1922), Geze (1943), Wantim, 2011
28 June 1954 (three weeks)	Summit	~2750	Vulcanian	fresh lava (basalt), Gases, tephra, bombs	-	-	De Swardt (1956), Wantim (2011)
6 February 1959 (22-30 days)	NE flank (2 sites)	~1961(1) 1500(2)	Strombolian and Hawaiian	Lava (aa), gases, tephra	~34	NE flank (towards Ekona)	Jennings (1954), Njome et al. (2008)
16 October 1982 (~24 days)	SW flank	~2700	Strombolian and Hawaiian	Lava (aa), gases, tephra	~10	Towards the coast	Fitton et al. (1983), Wantim (2011)
28 March 1999 (26 days)	SW flank (2 sites)	~2650(1) 1500(2)	Strombolian and Hawaiian	Lava(aa, Pahoehoe), gases, tephra	~5.1(site 1) ~60 (site 2)	Towards the coast (Bakingili)	Suh et al. (2003)
28 May 2000 (close to two months)	Summit & SE flank (2 sites)	~4095(1), ~2700 (2) ~3300 (2)	Strombolian and Hawaiian	Lava(aa, Pahoehoe), bombs,gases,tephra	~6 (site 2)``	South and SE towards Buea and environs	Suh et al. (2003, Ateba et al., 2009)

The 1982 eruption started on 16th October on the SW flank of the volcano and produced basanite lava and ash from an ancient cinder cone situated along a NE- SW trending fissure (~1 km long) at a height of approximately 2700 m (Fitton, 1983; Deruelle et al, 1987). Lava entered the forest and finally covered a distance of about 7.5 km and an area of 2.6 x 10^6 m^2 (Wantim, 2011). In a recent study, the morphology of the lava flow was described (Wantim, 2011) while its petrology and geochemistry have been done by Suh et al. (2003) and Njome et al. (2008). This eruption was accompanied by seismic swarms, felt in the regions of Buea and Bokosso (Ubangoh et al., 1997).

In March 1999, another volcanic eruption was recorded from two sites on the SW flank of Mount Cameroon. Mostly explosive activity started on the 28 March at site 1 situated at ~2650 m altitude, followed on the 30 March by the emission of lavas from site 2 at ~1400 m of altitude (Deruelle et al., 2000; Ateba et al., 2009; Table 3.1). The major flow from site 2 moved towards the coast onto the major road linking Limbe and Idenau at Bakingili and stopped ~200 m from the sea, after destroying forests and palm plantations on its path (Suh et al., 2003, 2011). Seismic activities recorded for this eruption started as far back as 1986 with a series of earthquakes events (felt in and around Bokosso and Buea areas) and caused a major explosion in May 1989 on the NW flank of the volcano (Ubangoh et al., 1997; Ateba et al., 2009). This eruption has been extensively studied for its morphology, petrology and geochemistry (Deruelle et al., 2000; Suh et al., 2003, 2011).

The level of local seismicity remained high after the 1999 eruption culminated in a violent explosion earthquake (large tectonic earthquake with an explosion sound) in May 2000 that marked the beginning of the 2000 eruption (Suh et al., 2003). This eruption occurred at two sites: site 1 (at the summit ~4095 m) with exclusively explosive eruptions and site 2 (~ between 2700 and 3300 m) with emission of lava that flowed towards the Buea region (Suh et al., 2003). An earthquake swarm during the 2000 eruption originated beneath the summit region (below the Moho ~ 20 km deep), suggesting the existence of a vertical magma conduit feeding the Mount Cameroon eruptions (Ateba et al., 2009). The 2000 eruption is seen as a continuation of the 1999 eruption due to the persistence of the seismic activity between the period separating the two eruptions, the similarities in the eruption behaviour and the composition of the lava produced (Suh et al., 2003).

Figure 3.4: Topographic contour of the Mount Cameroon Volcano displaying the historical lava flow with the corresponding eruptive year (modified from Suh et al., 2011 and Wantim, 2011).

A common phenomenon observed for all these historical eruptions is that they are usually associated with an increase of seismic activities and lava (except for the 1959 eruption) and are erupted along a ~1.5 km-long fissure orientated NE-SW formed from the shear zone within the underlying basement (Gèze, 1953; Njome et al., 2008, Favalli et al., 2012). Furthermore, eruptions often occur at more than one site. The sites at higher elevations are more explosive, while the lower elevations sites are characterised by emission of large volumes of lava (e.g. 1922, 1959, 1982, 1999, 2000; Suh et al., 2003, 2011; Ateba et al., 2009; Ubangoh, 1997).

The magma composition evolved differently with time i.e. varied from one eruption to another (Suh et al., 2003). The morphology of the cinder cones and explosion craters reveals that most eruptions have been of Strombolian type, though Hawaiian and Vulcanian types are also present (Gèze, 1953; De Swardt, 1956).

3.3 Risk assessment and lava flow hazard map

The lower flanks of the volcano represent a great economic resource of Cameroon due to the fertile soil. About 500,000 people live around Mount Cameroon with the greatest concentration at the south western flank (Buea with ~90,000 citizens and Limbe with ~85,000 citizens).

Detailed lava flow hazard and risk assessment studies around Mount Cameroon volcano were lacking until recently and research on this topic only started few years ago (Bonne et al., 2008; Thierry et al., 2008; Favalli et al, 2011; Wantim; 2011). Inhabitants living around the volcano are exposed to many natural risks, e.g. volcanic eruptions (explosive with pyroclastic fallout and effusive with lava flows), earthquakes, lahars and landslides (Thierry et al., 2008).

The map in Figure 3.5 represents the probability of lava invasion upon an occurrence of an eruption and derives from a statistical study of different geological phenomena likely to occur around Mount Cameroon (Thierry et al., 2008).

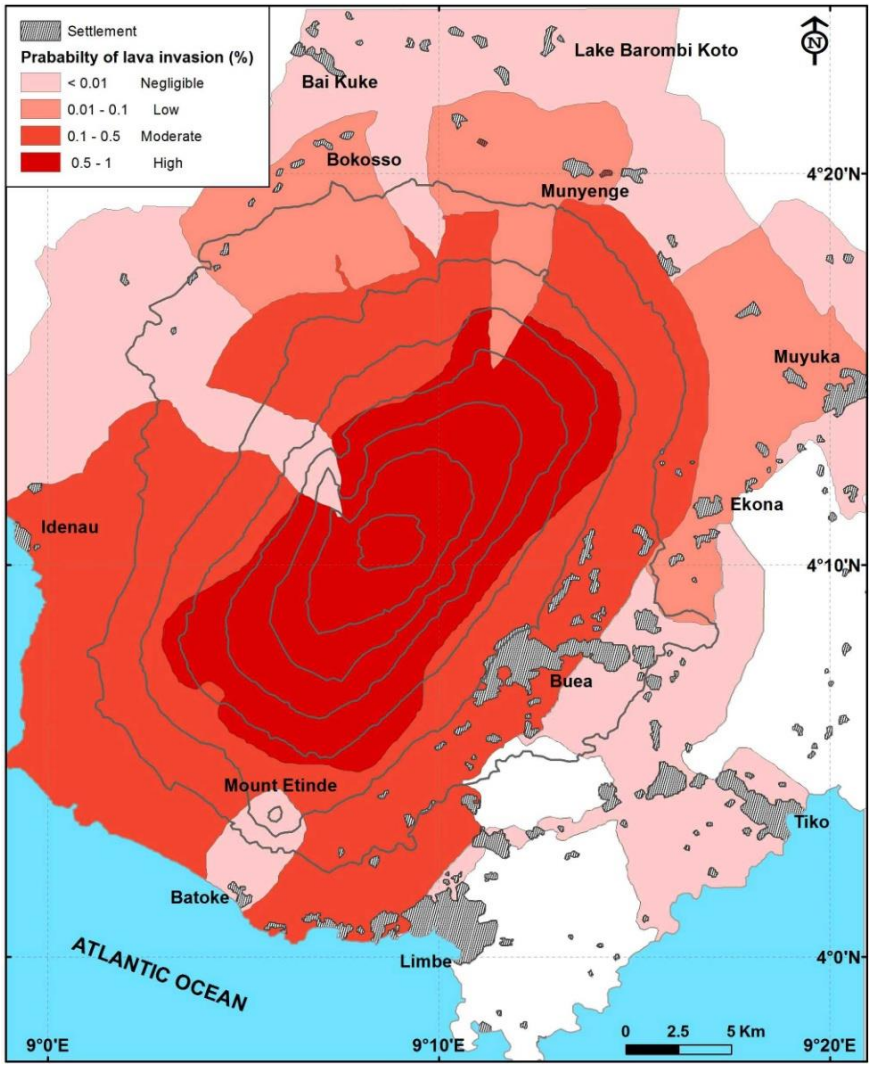

Figure 3.5: Lava hazard map of Mount Cameroon showing the human settlement (Thierry et al., 2008).

The lava flow hazard assessment takes into account the morphology, the frequency, the distribution and the average length of lava flows from previous eruptions. In general, the coastal and NE portions of the volcano are highlighted as being exposed to lava flow inundation whereas Mount Etinde acts as a barrier of lava flow invasion, hence making Batoke village safe from lava flow inundation (Thierry el., 2008; Favalli et al., 2011).

Chapter 4

Materials and Methodology

4.1 Seismic hazard parameters of Mt. Cameroon volcano

4.1.1 Earthquakes database

Seismic data used in this study are both historical and instrumental data compiled from various sources covering the 4ºN, 8.5º E and 5º'N, 10ºE for the period 1907 to 1991. The area mostly covers the Mt. Cameroon region. Report earthquakes event were taken from available published seismological bulletins and accepted thesis (Ambrasey & Adams, 1986; Ambey, 1989; Bertil, 1991). The compiled catalogue is incomplete in terms of historic events and complete during two periods of time (1985-1987 and 1975-1991). Hence the catalogue is split into an incomplete part (historic) and two complete parts corresponding to the instrumental information (Table 4.1).

Table 4.1: Summary of the input data for the seismic hazard assessment of Mt.Cameroon.

	Extreme part of the catalogue	**Complete part of the Catalogue**	
		Sub-catalogue #1	Sub-catalogue #2
Time period (dd/mm/yy)	16/11/1907-28/06/1954	23/11/1985-06/04/1987	02/11/ 1975-20/09/1990
Total number of events	6	288	5
Threshold magnitude	3.5	2.77	4.06

4.1.1.1 Historical data (1907-1954)

The main source for data of historical earthquakes in Cameroon has been established by Ambraseys & Adams (1986). For the period 1906-1954, six earthquakes of M_S magnitudes ranging from 3.5 to 4.5 were felt in Cameroon originating from Mount Cameroon (Table 4.2) and constitute our input data for the historical catalogue.

Table 4.2: Mt. Cameroon historical seismic catalogue; M_S is the surface wave magnitude (Ambraseys and Adams (1986).

Date	Lat. (°N)	Long. (°E)	M_S
16 Nov. 1907	4.6	9.6	4
17 Dec. 1908	4	9.7	4.3
26 Apr. 1909	4.3	9.4	4.5
23 Feb. 1910	4.2	9.1	3.5
3 Feb. 1922	4.2	9.1	3.5
28 Jun. 1954	4.2	9.2	3.5

4.1.1.2 Instrumental data

The first seismic station in Cameroon was installed in 1982 (Fairhead, 1985). The instrumental data used in this study originates from two different sources and therefore, will be named sub-catalogue #1 and sub-catalogue #2.

i) Sub-catalogue #1 (1985-1987)

This catalogue was produced by Ambey (1989) while studying the seismotectonic activities of Mt. Cameroon using temporal and permanent seismic stations installed around the volcano. The overall seismicity during this period is characterised by the predominant clustering of earthquakes at a few distinct localities (representing earthquake swarm regions or regions of continuous occurrence of single earthquakes).Focal depths extend from near surface to about 55 km, indicating the presence of both crustal and subcrustal activity. Errors in hypocentral parameters are estimated with a 95% confidence level. In particular, location accuracies of the seismic events are between about ± 3 km and ± 5 km for the Epicentral coordinates and the focal depths respectively depending on how far detected events are from the seismic network (Ambey, 1989). Four major seismic source zones are identified as follows:

- Region A: The northwest Seismic Zone

Earthquakes in this region occurred both as discrete and swarm events. The concentration of events around Bokosso represents the Bokosso swarm (Fig. 4.1). Focal depths studies reveal that events are relatively shallow less than 20 km deep, with no obvious linear trend of epicentres. The Bokosso swarm was a short, intense swarm that started on the 13 February 1986 and lasted for 10 days.

- Region B: The southeast seismic zone

This part of the volcano represents the most seismically active area of the Mount Cameroon region (Fig. 4.1). The depth distribution of these events reveals that they are relatively deep, extending from about 30 km to 55 km and maybe shallower northwards, towards Ekona (Ambey, 1989). Events usually occurred as single shocks about once every three days of which some are accompanied by one or two aftershocks. The fact that this area is close to the equator, suggests that these seismic events might be triggered by the earth-tide, but no correlation was found (Ambey & Fairhead, 1991).

- Region C: Offshore Bimbia Seismicity

Almost all earthquakes located in this region occurred during the period 1985/86. This area appears to be characterised by episodic burst of swarms rather than an area of continuously occurring activity. A swarm started on the 25 February 1986 and lasted for about 6 days. The

earthquakes epicentres roughly define an E-W trend (Fig. 4.1) with focal depth between 13 and 22 km (Ambey, 1989).

- Region D: Wouri - Douala area

The small concentration of earthquakes around the Douala region (Fig 4.1) was observed as a sequence of two minor swarms. Some events are also scattered in the Wouri estuary and around the coastal boundary. The focal depths for these events range between 20 and 30 km.

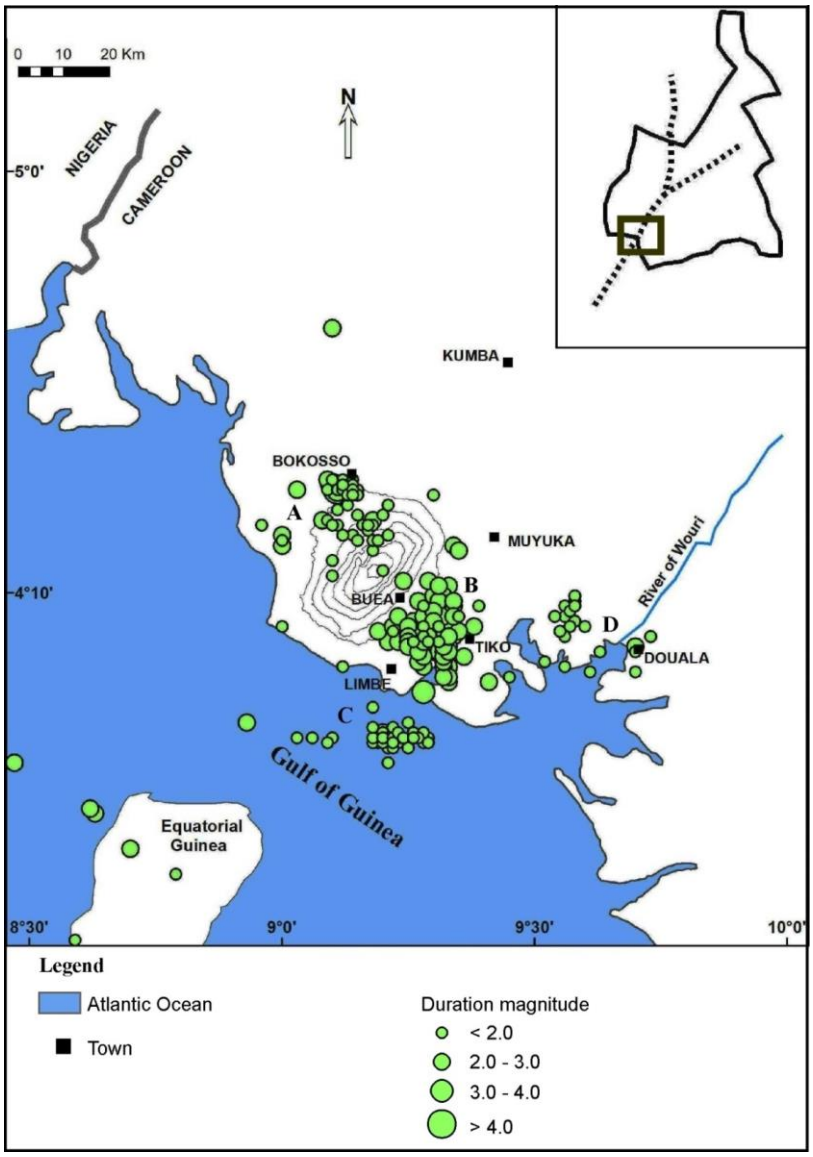

Figure 4.1: Epicentre map for the period 1985 to 1987. The identified seismic zones for the analysis are shown by the letters A, B, C and D (Ambey, 1989).

ii) Sub-catalogue #2 (1975-1991)

For his PhD thesis, Bertil (1991) studied the intraplate seismicity of West Africa using data from Lamto Geophysical station in Cote d'Ivoire situated ≈1500 km from Cameroon. A seismic swarm of 6 events with duration magnitude of about 4 originated from the Mt. Cameroon region between the 2nd and the 7th of November 1975.] A similar swarm occurred on the 13 February 1986 with five events of duration magnitude between 3.7 and 4.2. This swarm was detected by Mt. Cameroon stations (Ambey, 1989) and is discussed in section 4.1.1.2(i). Consequently, those events are removed from this sub-catalogue to avoid duplication. Three other earthquakes originated from Mt. Cameroon region from 1989 to 1991. However, due to the fact that Mt. Cameroon is situated at the limit of the detection zone which is between 400 and 1200 Km from the seismic station, the location and size of some of those earthquakes was uncertain. In total, only five seismic events were fully detected in terms of location and sizes and constitute the sub-catalogue #2 (Table 4.3).

Table 4.3: Mt.Cameroon instrumental sub-catalogue for the period of 1975 to 1991; M_D is the duration magnitude (Bertil, 1991).

Date	Latitude	Longitude	M_D
02 Nov. 1975	4.73	9.25	4.3
05 Nov. 1975	4.65	9.35	4.2
06 Nov. 1975	4.64	9.33	4.1
01 Jun.1989	4.39	9.14	4.2
20 Sep. 1990	4.37	9.31	4.2

4.1.2 Method

4.1.2.1 Homogenisation of the magnitude of the earthquake catalogues

The size of an earthquake can be defined using different magnitude scales depending on the stations used by the seismological centres when determining the source parameters. As a result, some significant discrepancies may be observed in reported earthquakes. Therefore, it is necessary to choose a suitable magnitude scale to homogenise the catalogue prior to a seismic study. The moment magnitude is selected for the unification of the catalogue since it is directly linked to the seismic moment which is important to characterise an earthquakes source (Joyner, 1984). However, for small earthquakes local magnitude M_L gives a better measure of the size of an earthquake (Singh, 1990).

To convert corresponding seismic events of magnitude M_S in the extreme catalogue into the moment magnitude M, the following empirical equations were applied (Scordilis, 2006):

$$M = 0.67(\pm 0.005)M_s + 2.07(\pm 0.03) \qquad 3.0 \leq M_s \leq 6.1$$

Ambey (1989) established a relationship between the Richter Local Magnitude M_L and the magnitude from signal duration M_D (Fig. 4.2):

$$M_D = M_L \tag{4.1}$$

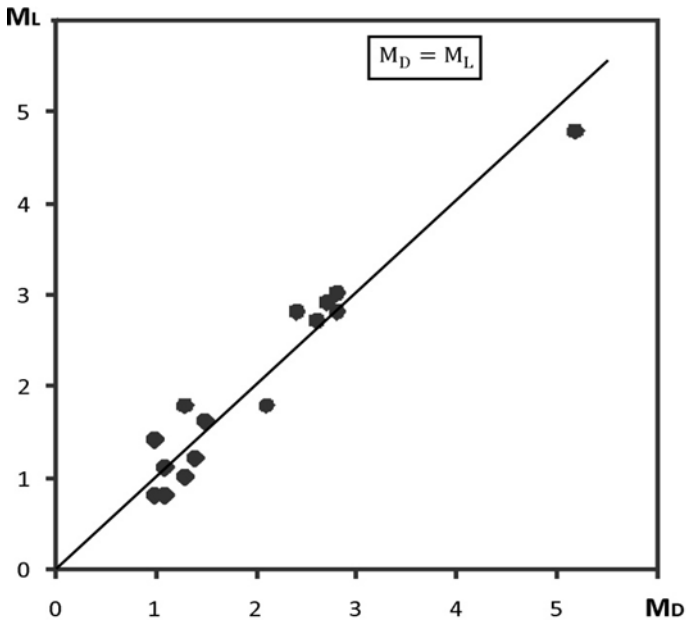

Figure 4.2: Correlation between M_D and M_L data (Ambey, 1989).

Hanks and Kanamori (1979) shows that the local magnitude M_L and the surface wave magnitude M_S are connected to the moment magnitude M via the seismic moment M_0 through the following equations

$$\log_{10} M_0 = 1.5\, M_s + (16.1 \pm 0.1) \tag{4.2}$$

$$\log_{10} M_0 = 1.5\, M_l + 16.0 \tag{4.3}$$

$$M = 2/3 \log_{10} M_0 - 10.7 \tag{4.4}$$

where M_0 is the seismic moment in dyne.cm; these relations are valid for $3 \leq M_L \leq 7$ and $5 \leq M_S \leq 7.5$

However, these relations were extended for $M_L \leq 3$ to unify the magnitude of the sub-catalogue #1 from Ambey (1989) since the coda duration magnitudes $M_D$are linked to M_l (Hanks and Kanamori, 1979; Fig. 4.2).

To correlate the duration magnitude M_D and the local magnitude M_L referenced in the instrumental sub-catalogue #2, a linear regression was done based on events where both M_D and M_L and the following relation was used (Fig. 4.3).

$$M_L = 1.28M_D - 1.19 \quad (4.5)$$

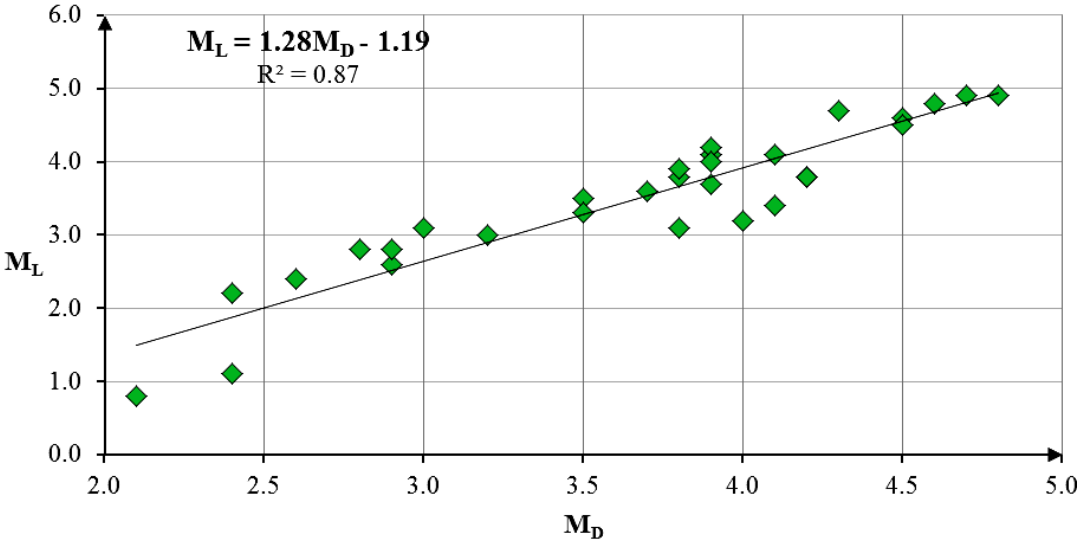

Figure 4.3: Linear regression of values of M_L versus M_D of selected events observed in West Africa from 1965 to 1991(compiled from Bertil, 1991).

4.1.2.2 Completeness of the catalogues

The statistical distribution of a magnitude for a group of earthquakes follows the Gutenberg-Richter (1954) frequency-magnitude relationship:

$$\mathrm{Log}_{10}N(\mathrm{M}) = a - b\mathrm{M} \quad (4.6)$$

where N is the number of earthquakes of magnitude M or greater, a and b are constants. The completeness of the catalogue is defined as the range over which the magnitude-frequency relation roughly follows the Gutenberg-Richter relationship. The most common approach used to determine the threshold magnitude is by plotting the cumulative number of events against earthquake magnitude. Each value in a cumulative quantity depends on all of the preceding values, thus it is important to also plot the non-cumulative FMD in addition to the cumulative FMD. The level of completeness is determined using the maximum curvature technique (Wiemer and Wyss, 2000). This technique is a straightforward method and consists in defining the point of the maximum curvature by computing the maximum value of the first derivative of the frequency-magnitude plot. In practice, this matches the magnitude bin with the highest frequency of events in the non-cumulative FMD. The advantage of this method is the fact that it requires fewer events than other techniques.to reach a stable result. Hence found suitable to determine

M_{min} since the total number of events is relatively small. It should be noted that only deviations from the G-R linearity at the lower end of the FMD are considered rather than deviations at upper end of the FMD which can lead to under-sampling (Mignan and Woessner, 2012; Woessner and Wiemer, 2005).

In fact, instrumental sub-catalogue #1 contains a gap period of ≈ 9 months. To verify the quality of the data in terms of acquisition and processing, two assumptions are made. The first one (case I) considers the gap and splits the data into two complete sub-catalogues, and the second assumption (case II) treats it as one complete sub-catalogue.

Figure 4.4 and 4.5 represent the cumulative and non-cumulative frequency-magnitude plots in case I. The gradual curvature in FMD plots is commonly due to (1) the spatiotemporal evolution of the seismic network (2) potentially man-made effect such as the use of different magnitude scaling relationship and (3) physical processes in the earth (Mignan and Woessner). In the case of Mt. Cameroon volcano, 95 % of events of the sub-catalogue in case I are of duration magnitude less than 3. This is typical to volcanic environment with the predominant occurrence of swarms of small magnitudes and might explain why the FMD catalogue (Fig.4.4) does not strictly follow the G-R law. From the maximum curvature method describe above (Wiemer and Wyss, 2000), the threshold magnitude corresponding to case I is around 2.7 as highlighted by the arrows (Fig 4.4 and 4.5). Similarly, the threshold magnitude in case II is also around 2.7 (Fig. 4.6).

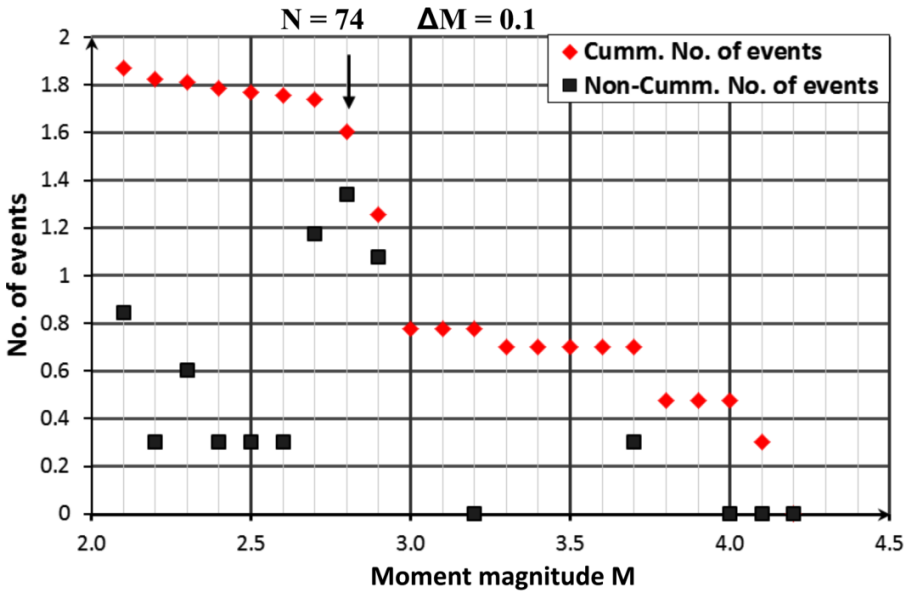

Figure 4.4: Cumulative and non-cumulative FMD on logarithmic scale of earthquakes that occurred during the period 1985-1986. The arrow indicates the level of completeness M_{min} and the magnitude increment ΔM = 0.1.

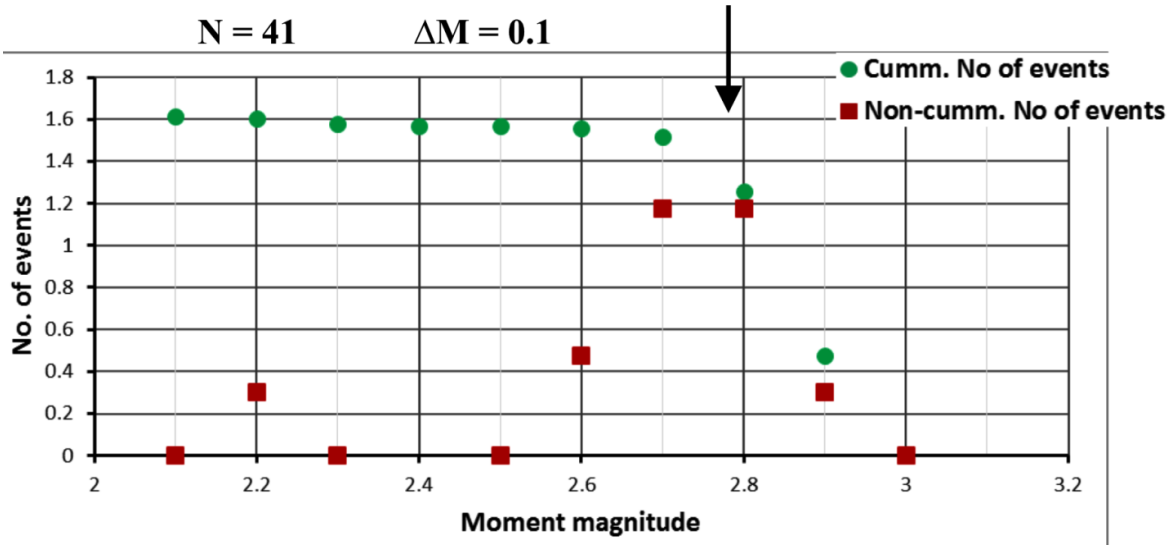

Figure 4.5: Cumulative and non-cumulative FMD on logarithmic scale of earthquakes that occurred during the period 1986-1987. The arrow indicates the level of completeness M_{min} and the magnitude increment ΔM = 0.1.

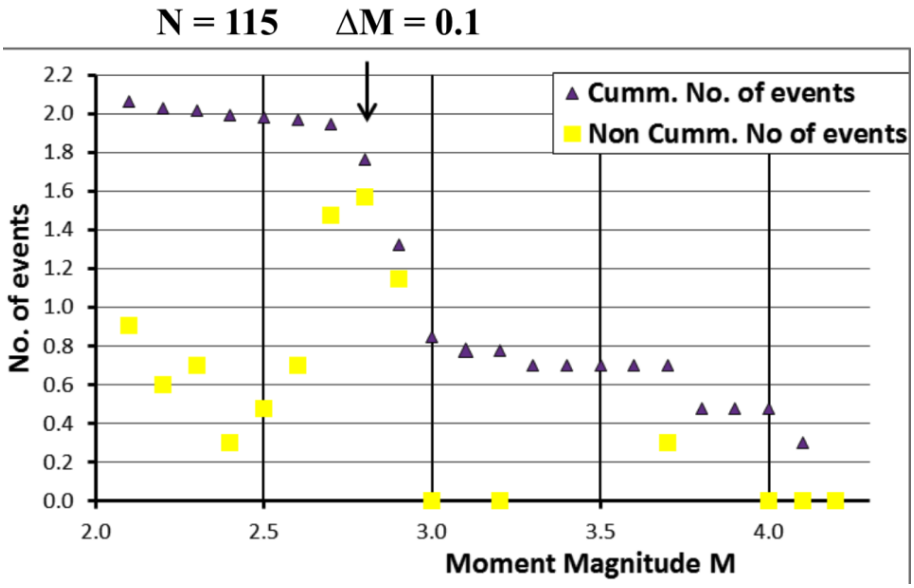

Figure 4.6: Cumulative and non-cumulative FMD on logarithmic scale of earthquakes that occurred during the period 1985-1987. The arrow indicates the level of completeness M_{min} and the magnitude increment ΔM = 0.1.

In the absence of seismic network as prior 1982 in Cameroon, the threshold magnitude of the historical catalogue will be the lowest magnitude at which an earthquake can be felt. In the compiled historical catalogue, all earthquakes were reported to have been felt in and around the Mt. Cameroon region, thus the level of completeness of the historical catalogue can be assumed to be M_s = 3.5.

Similarly, the seismic signals detected by the Lamto network stations could only be localised for duration magnitude greater than or equal to 3 (Berlil, 1991). For that reason, the magnitude of completeness of the sub-catalogue #2 is taken as the lowest duration magnitude of the compiled catalogue i.e. $M_d = 4.1$

4.1.3 Mean annual activity rate λ and b-value

To evaluate the seismic hazard parameters, a well-known technique (Kijko and Sellevoll, 1989; 1992) was used. In this approach, it is assumed that the earthquake catalogue contains two types of data: macroseismic observations of events that occurred over a period of the last few hundred years and a complete recent dataset for a relatively short period of time. The theory behind this method is well described in chapter 2 (section 2.2.2).

Table 4.4: Required format for the input files

Format of the historic file		Format of the complete files	
Start of the catalogue (YY MM DD)		Start of the catalogue (YY MM DD)	
End of the catalogue (YY MM DD)		End of the catalogue (YY MM DD)	
Threshold magnitude		Threshold magnitude	
Magnitude uncertainty		Magnitude uncertainty	
Event date(YY MM DD)	magnitude	Event date(YY MM DD	magnitude
…	…	…	…
…	…	…	…

The MATLAB computer program HA2 developed from this method and written by Kijko and Sellevoll (1989; 1992) is used for the analysis. The input of the program consists of three files containing the seismic data of the Mt. Cameroon area: one containing historic events and two completed catalogues. In both historic and instrumental data files, it is important to specify the level of completeness, the standard error in the determination of the catalogue and the span of the catalogue (Table 4.4) In general, the format of the historic files contains two columns (dates and magnitudes) and the format of the complete files only has one column of magnitude.

The code requires the knowledge of *a-priori b*- value corresponding to the type of seismicity induced area (volcanic or tectonic). As output, the code calculates the average value of the mean activity rate λ, the Gutenberg-Richter *b*-value and produces hazard curves of the area under investigations.

4.1.4 Maximum possible earthquake magnitude

The maximum magnitude m_{max} is sometimes inferred through other available information such as the geology and paleoseismicity. Since there is no well-documented information about the faults and paleoseismic events of Mt. Cameroon, a procedure for the evaluation of m_{max} developed by Kijko & Sellevoll (1989; 1992) and Kijko (2004) was used based on equations derived from Cooke (1979). This procedure considers that m_{min} is known, only depends on seismic data, and is therefore, free from subjective assumptions. Section 2.2.3 (Chapter 2) illustrates some methods used in the determination of m_{max}. Several statistical techniques for assessing the value of m_{max} have been compiled by Kijko & Singh (2011). The described procedures include parametric and non-parametric methods and are computed in a MATLAB toolbox called MMAX written by the latter authors.

The compiled seismic catalogue is divided into an incomplete part (historic) and two complete parts, each with a different level of completeness. The format of the input file used for MMAX toolbox simply consists of a column of magnitudes. For non-parametric approaches, the estimation of the probability density function requires the knowledge of a smoothing factor *h.* In the absence of a seismic event catalogue, the *b*-value of the Gutenberg-Richter and its uncertainty, the mean activity rate and its uncertainty, the levels of completeness, the time span of the catalogue, the maximum observed magnitude in the area and its uncertainty are required.

The code generates information about the input data and estimated the maximum magnitude with their respective standard deviations using several methods (parametric and non-parametric) including the three methods described in Chap. 2. Standard errors of maximum observed magnitude were arbitrarily chosen equal to 0.3.

4.1.5 Standard deviation of the determination of magnitudes and *a-priori b*-value

The standard deviations in the magnitude determination of our catalogues were assumed to be 0.3 for the historical catalogue, 0.2 and 0.3 for instrumental sub-catalogue #1 and sub-catalogue #2, respectively. To improve the standard deviation of the annual activity rate, the time span of each catalogue stretches from one month before the first seismic event until one month after the last seismic event. Since Mt.Cameroon is a volcanic area, the average *a priori b*-value is taken to be 1.5 ± 0.2 (Kijko, personal communication, 2015).

4.2 Rate of recurrence of volcanic eruptions of Mt. Cameroon

4.2.1 Data

In total, 16 eruptions were confirmed to have originated from Mt. Cameroon volcano between 1800 and 2000 (Table 4.5). The last volcanic eruption of Mt. Cameroon took place over 15 years ago. In an assessment of the volcanic hazard, it is important to evaluate the rate of occurrence of volcanic eruptions using an appropriate method.

Table 4.5: Authenticated dates of eruptions of Mt. Cameroon Volcano for the period 1800-2000 (Lapi et al., 2010).

Years of eruption	Interval between Eruption (years)
1800	
1815	15
1835	20
1838	3
1845	7
1865	20
1866	1
1868	2
1909	31
1922	13
1925	3
1954	29
1959	5
1982	23
1999	17
2000	1

Fig 4.7 represents the trend analysis of the total number of eruptions that have occurred at Mt. Cameroon throughout the time. A quick inspection of this figure indicates that Mt. Cameroon's eruption frequency remains relatively constant with time. This means that volcanic eruptions occur randomly (Lapi et al., 2010), which makes a simple Poisson distribution suitable for Mt. Cameroon volcano eruptions.

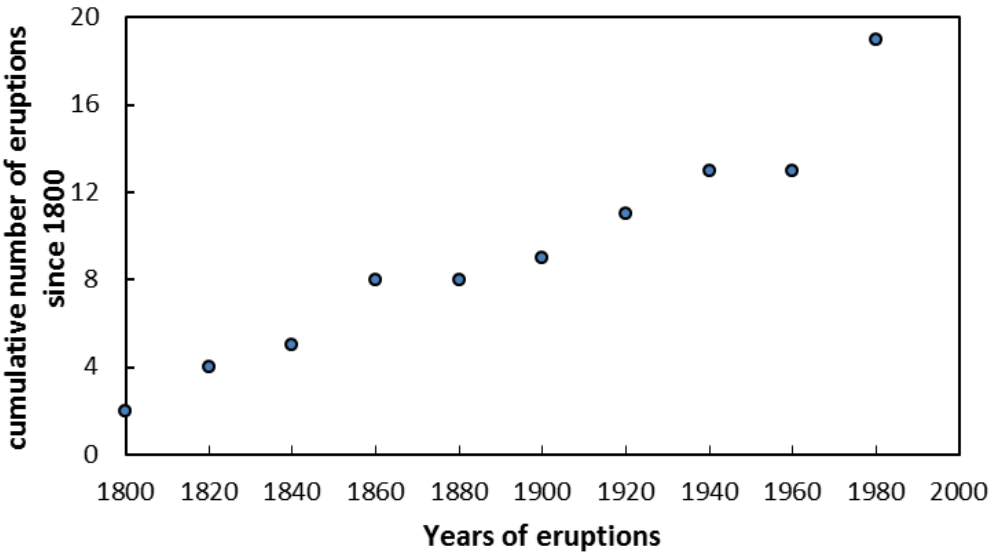

Figure 4.7: Scatter plot of Mt. Cameroon eruption since 1800.

4.2.2 Determination of the rate of eruption occurrence λ

In this section, the two different methods described in section 2.3 of Chapter 2 were applied.

Following the relation derived by Ho et al.; (1991), the rate of recurrence of eruption is equal to:

$$\hat{\lambda} = \sum_{i=1}^{n} \frac{x_i}{n} = \bar{x} \tag{4.7}$$

where $x_1, x_2 \ldots x_n$ represent the observed frequency of eruption and n is the length of time corresponding to all the eruptions that have ever occurred .

Numerically,

$$\hat{\lambda} = \frac{16}{(2015 - 1800)}$$

$$\lambda \simeq 0.07442$$

Following the equation developed by Jones et al., (1999), the rate of eruptions at Mt.Cameroon is given by:

$$\lambda = \frac{J}{(Z + \sum_j^J Y_j)} \tag{4.8}$$

where Z is the time (in years) since the last recorded eruption, Y is the time interval between two recorded eruptions and J is the total number of recorded eruption. From the eruption dates mentioned above (Table 4.5), it can be written:

$$\lambda = \frac{16}{15 + (2000 - 1800)}$$

$$\lambda \simeq 0.07442 \text{ eruption/year}$$

It is observed that when all eruptions are dated (as in the case of Mt. Cameroon), λ is given by the total number of eruptions divided by the considered time frame. In this case, Equation (4.8) derived by Jones et al.; (1999) and equation (4.6) from Ho et al.; (1991) are equivalent.

Chapter 5

Results and Discussion

Seismic and volcanic hazard parameters are important, firstly because they are needed in the overall evaluation of the hazards caused by a particular volcano. Secondly, they can, to a certain extent, be of major significance to the problem of volcanic eruption forecasting. Statistical methods were applied to the seismic and eruption data, recorded at Mt. Cameroon volcano. Results of the hazard analysis are displayed as seismic hazard curves of return periods of 25, 50 and 100 years. It was found that eruptions occur at Mt. Cameroon at an average rate of 13 years and the map of probabilities of eruption was derived.

5.1 Seismic hazard parameters

5.1.1 Seismic activity rate λ and *b*-value of Gutenberg-Richter

The region around Mt. Cameroon is seismically very active. The earthquakes are relatively shallow in nature with depth extending from near surface to about 55 km (Ambey, 1989). The largest earthquake of moment magnitude 5.09 ± 0.3 occurred in 1909.

Table 5.1: Seismic Hazard parameters of the Mt. Cameroon region for m_{min} =2.77; λ is the mean activity rate, β=b ln10 and b-value is the Gutenberg-Richter parameter. SD is the standard deviation.

	Case I (± SD)	Case II (± SD)
λ(year)	32.528 ± 5.640	20.594 ± 4.027
β	3.52 ±0.04	3.52 ± 0.05
b-value	1.53±0.02	1.53 ± 0.02
Mmax	5.34±0.77	5.34±1.55

The MATLAB computer program HA2 has been applied to our catalogues and the results are computed based on a method implemented by Kijko and Sellevoll (1989, 1992) with 25% expected uncertainty of parameters of the seismicity model. Since instrumental sub-catalogue #1 has a gap period of nine months (when seismic stations were not operating), two assumptions were made: (1) the sub-catalogue #1 was split into two complete sub-catalogues, (2) the gap period was ignored and the seismic events were gathered in one complete sub-catalogue. In case I, seismic data reported in Ambey' thesis, (1989) were divided into two complete specific time frames: from 1985 to early 1986 and between late 1986 and early 1987. In case II, the sub-

catalogue #1 is assumed to be completed for the entire period of 1985=-1987. Results from the assumptions made in case I and case II respectively are presented in Table 5.1

In general, the maximum magnitude obtained from case I is more accurate than the one obtained from case study II. The computed Gutenberg-Richter value for the Mt. Cameroon area is in both cases b = 1.53 ± 0.02. This value agrees with observations from other volcanic areas where the b-value usually is greater than 1 (Bridges & Gao, 2006; Mc.Nutt, 2005; Farrell et al., 2009). The mean activity rate $\lambda(m_{min} = 2.77)$ in the first assumption is higher than the value obtained in the second case (Table 5.1). The fact that the gap period in case study I was removed, the time span of the catalogue has reduced, which results in an increase of the mean activity rate.

From Figures 5.1 (i) & (ii), it is clear that events of greater magnitude (≥ 4.5) have higher return periods, implying that weaker events occur more frequently. This observation is confirmed by our instrumental sub-catalogue #1 where most earthquakes have magnitudes ranging from 2.7 to 3.2. For the maximum magnitude m_{max} = 5.34, the return period is computed as 502 years

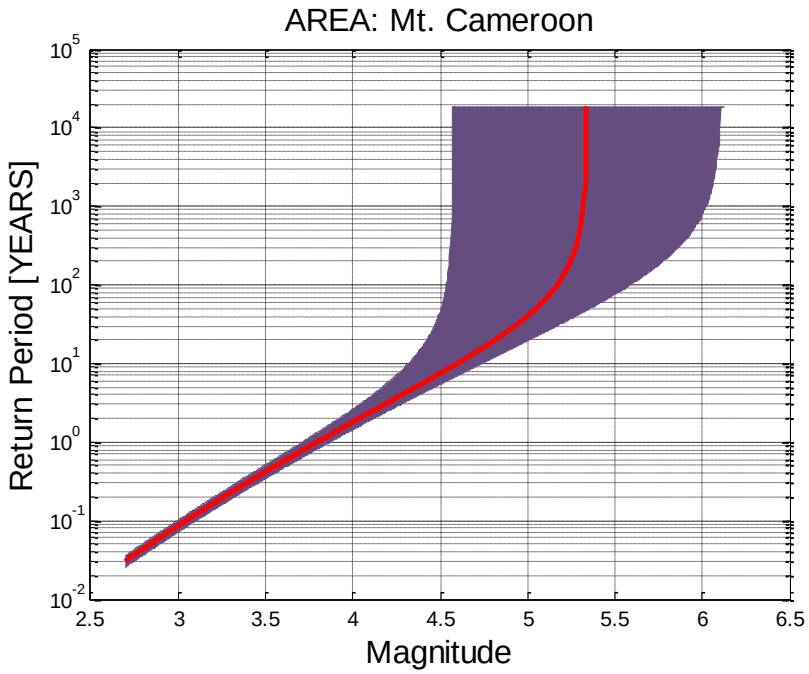

Figure 5.1 (i): Curve showing the estimated return period using mixed data in the case study I. The maximum possible moment magnitude is 5.34

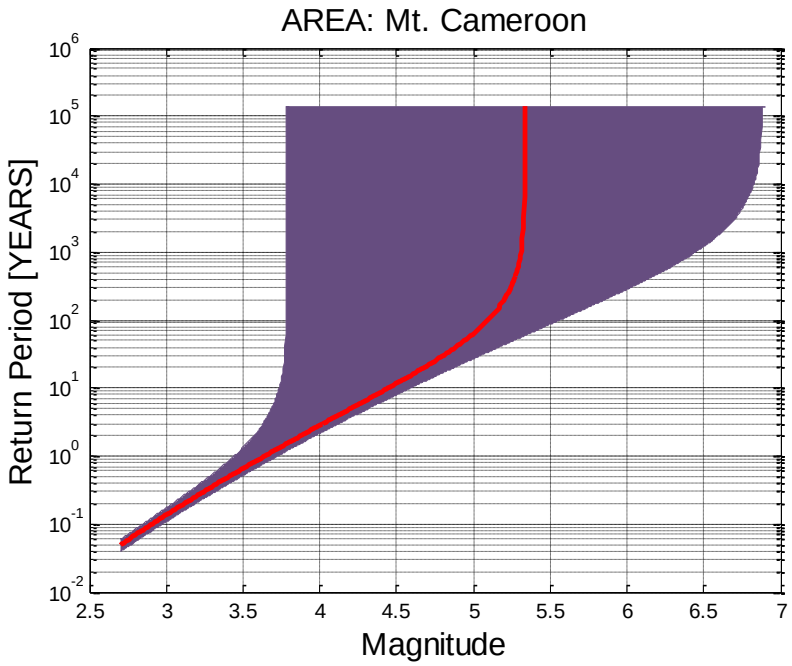

Figure 5.1 (ii): Curve showing the estimated return period using mixed data in the case study II The maximum possible moment magnitude is 5.34

Considering the respective annual probability of occurrence and for 25, 50, and 100 years return periods plots (Figs. 5.2 & 5.3) one can observe that the probability of occurrence of earthquakes decreases with magnitude.

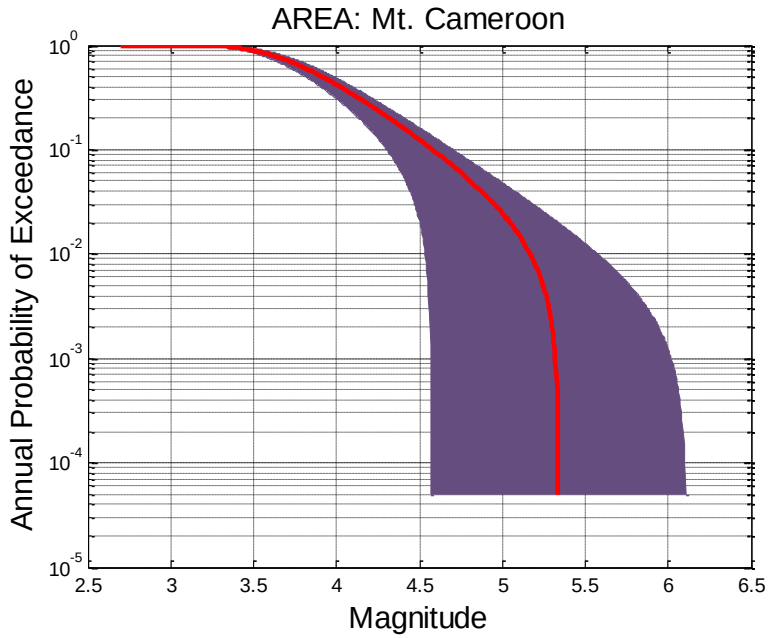

Figure 5.2 (i): Probability-magnitude diagram for one year return period for the case study I. The maximum possible moment magnitude is 5.34

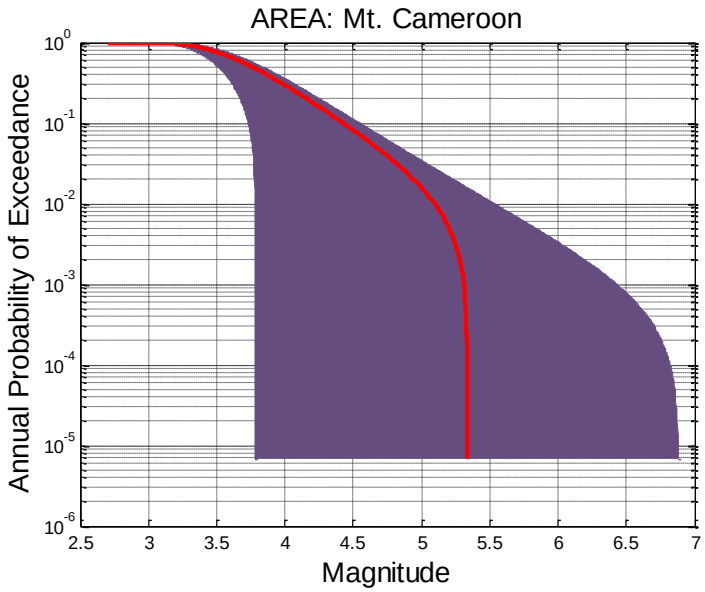

Figure 5.2 (ii): Probability-magnitude diagram for one year return period for the case study II. The maximum possible moment magnitude is 5.34

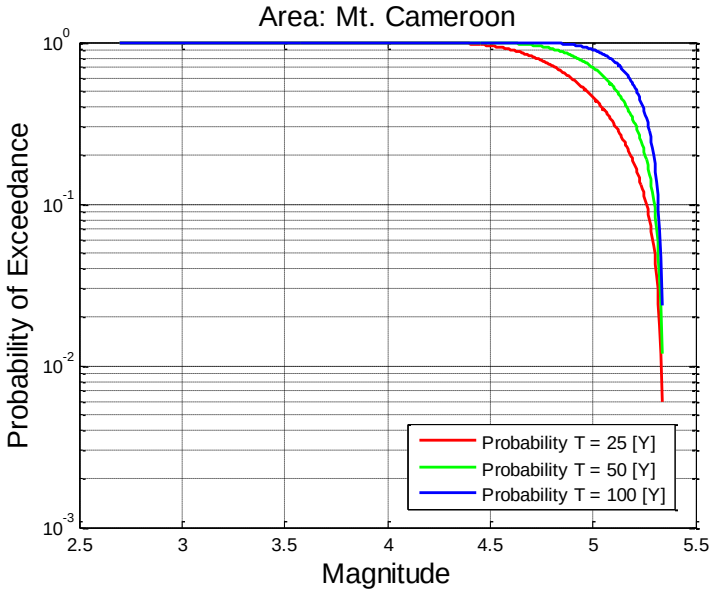

Figure 5.3 (i): Curve showing the probability-magnitude diagrams for 25, 50 and 100 years return periods following case study I.

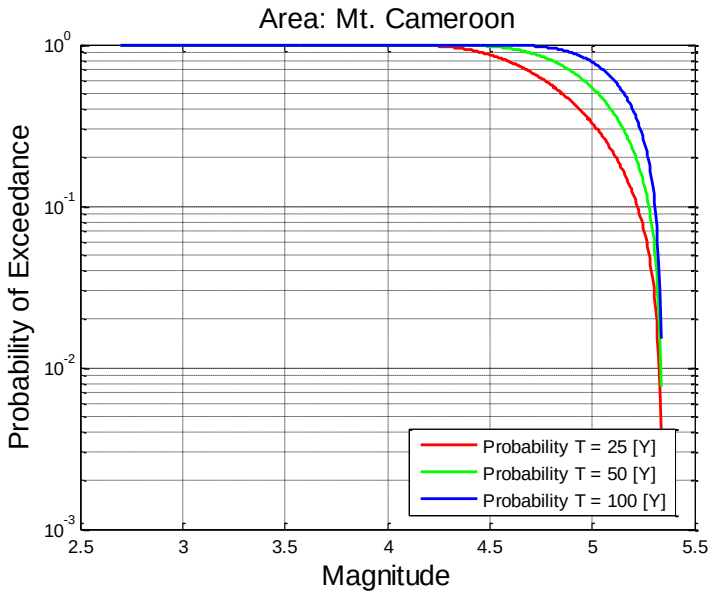

Figure 5.3 (ii): Curve showing the probability-magnitude diagrams for 25, 50 and 100 years return periods following case study II.

The parameter λ quantifies the number of events occurring per year. The results show that on average one seismic event occurs every 10 days. This is far less than the number of earthquakes that are actually being detected, i.e. one to two events every three days (Ambey et al., 1989). The parameter λ strongly depends on the time span of the catalogue. The seismic catalogue used in this report stretches on a longer period of time (≈ 84 years) compare to the seismicity period of observation from Ambey (1989), i.e. under two years. This could be the reason for the inconsistency in the value of λ.

The value of the maximum regional magnitude estimated according the K-S procedure is identical in both case I and II and is equal to 5.34. Nevertheless, the standard deviation is considerably higher when one assumes that instrumental sub-catalogue #1 is complete from the period 1985 to 1987.

Previous average b-values of Mt. Cameroon, obtained by the standard linear regression method include 0.69±0.07 and 0.86±0.06 for the period 1985/1986 and 1986/1987, respectively (Ambey, 1989). These results are not characteristic of volcanic areas, thus, the stress releases from earthquakes during these periods were associated with the tectonic setting even though the occurrence of swarms are usually triggered by the activity in the magma chamber (Ambey, 1989).

Nevertheless, the average *b*-value computed here is in accordance with the one derived by Ateba et al. (2009) who reported a *b*-value of 1.43 ± 0.02 from earthquake data events that occurred in

the Mt. Cameroon region during the year 2000. Since the *b*-value controls the capability of a medium to release the accumulated energy (Gibowicz & Kijko, 1994), one can suggest that the intrusion of the magma body could be responsible for the stress concentration. This generates the occurrence of relatively small earthquakes as observed in our instrumental sub-catalogue #1 and, thus, increases the *b*-values.

There are temporal changes of the seismic activity λ as well as the parameter *b* that, if disregarded, can lead to biased (over-estimated) values of the seismic hazard parameters (Kijko, 2004). It has been demonstrated that *b*-value parameter has a longer time constant in some volcanoes (years to decades; Mc.Nutt, 2005). In fact, the occurrence of earthquake swarms increases *b*-value to a short-lived high which then decreases to a of normal background level with a longer time constant. However, there is a spatial variation of the seismic activity rate and *b*-value beneath volcanic regions (McNutt, 2005, Bridges & Gao, 2006; Sánchez et al., 2005).

In the instance of Mt. Cameroon, this assumption could not adequately be verified because of (1) the absence of enough seismic data for the period of studies (2) the non-availability of the catalogue used in the study done by Ateba et al. (2009) and (3) the hypocentre depths of the data used in this study are not very accurate since the accuracies can greatly exceed 5 km (Ambey, 1989) The seismic catalogue combined for the study of Ateba et al. (2009) could have been analysed separately through the method used in this thesis (Kijko and Sellevoll, 1989; 1992) to show the temporal fluctuation of the seismic activity rate and the parameter *b* between 1984 (using the catalogue from Ambey, 1989) and 2000 (using the catalogue from Ateba et al., 1989). However, looking at previous activity rate and *b*-values (Ambey, 1989; Ateba et al., 2009), it can be speculated that variations of these seismic parameters is related to the volcano's eruptive activity.

Several factors can influence the reliability of *b*-value especially for volcanic areas. The predominance of a large number of small earthquakes swarms tend to increase the *b*-values and can affect the linearity of the FMD (Gibowicz & Kijko, 1994). Fortunately, such behaviour was not noticed in our instrumental sub-catalogues (see Fig. 4.6 in Chapter 4). Another factor that controls the *b*-values is the change in the number of seismic network coverage. This results in inconsistencies in magnitude reporting, which can affect the distribution of *b*-values (Bridges & Gao, 2006). This was verified by separating the instrumental sub-catalogue #1into two sub-catalogues (see Table 5.2) and no difference in the rate of earthquakes reported was observed since the obtained *b*-values are identical.

There are many possible causes for a higher than normal *b*-value at volcanoes. These include the relatively small number of large events compared to small events. For instance, of all

earthquakes recorded in our instrumental sub-catalogue #1, only two events had a magnitude as high as 4. The high material heterogeneity beneath Mt. Cameroon Volcano caused by the existence of highly fractured rock above the magma chamber (Sánchez et al., 2005) might be at the origin of a high *b*-value.

Another possible cause of the high *b*-value anomaly could be the stress regime in the magma chamber due to the exsolution of gases from fumaroles (vents around a volcano from which hot gases especially steam are emitted) as observed in most Mt. Cameroon eruptions (Wantim, 2011). The interaction between the rising magma and groundwater at shallow depth consequently reduces the stress level and allows the recurrence of small earthquakes which increase the *b*-values (Bridges & Gao, 2006).

5.1.2 Maximum regional magnitude

Table 5.2: Maximum magnitude of Mount Cameroon volcano estimated from different approaches.

	Procedures	**Estimated** m_{max}	**Standard deviation**
Parametric methods	Kijko-Sellevoll -APPROX. (K-S)	5.77	0.74
	Kijko-Sellevoll -EXACT (K-S)	5.76	0.74
	Kijko-Sellevoll-Bayes (K-S-B)	5.65	0.63
Non-parametric	Robson-Whitlock (W-R)	5.23	0.69
	Robson-Whitlock-Cooke (R-W-C)	5.16	0.48
	Non-parametric with Gaussian kernel (N-P-G)	5.21	0.32

The computer program MMAX described in section 4.1.4 of Chap. 4 is used to evaluate the maximum magnitude of a possible earthquake originating from the Mt. Cameroon region. The output file contains information summarised in Table 5.2. The observed cumulative number of earthquakes and its non-parametric fit for the Mt. Cameroon seismic data are shown in Fig. 5.4. The seismicity in the Mt.Cameroon region is characterised by the occurrence of earthquakes swarms of small magnitudes. The compiled catalogue used for the determination of the maximum magnitude comprises a column of magnitudes of events from both the extreme catalogue and the complete sub-catalogues. In general, the maximum regional magnitude values of the Mt. Cameroon area overlap when their standard deviations are taken into account. However, it can be noticed from the standard deviation that the non-parametric methods are substantially better than the parametric procedures.

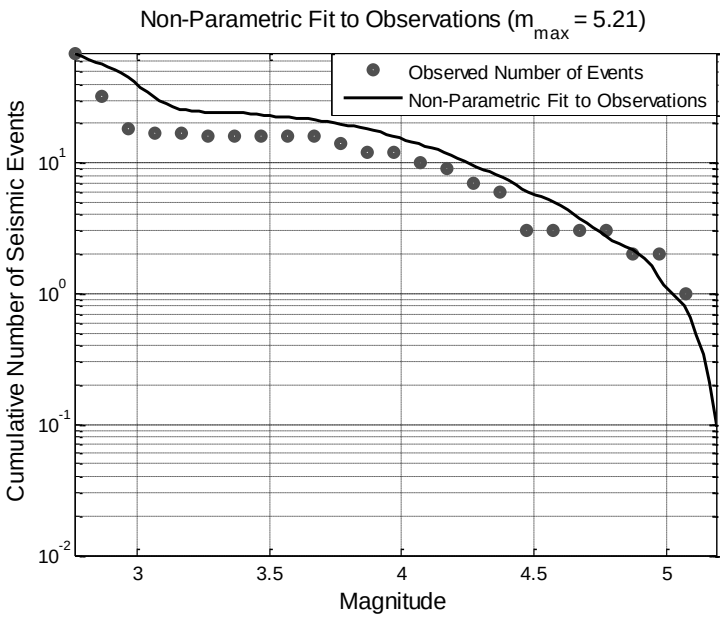

Figure 5.4: Plot of the observed cumulative number of earthquakes and the non-parametric fit of the Gutenberg-richter CDF for the data from the Mt. Cameroon region. The estimated value of m_{max} from the fit is equal to 5.21

Figs. 5.5 & 5.6 represent the maximum possible magnitude to be expected in the Mt. Cameroon region when the Gutenberg-Richter model is assumed to fit the magnitude distribution and Fig. 5.7 estimates m_{max} when no specification on the form of the magnitude distribution is required (non-parametric). The maximum observed magnitude is determined with a standard error assumed to be 0.3

These applied formalism plots also provide a confidence limit for the estimated m_{max} that gives an indicator on how reliable the estimated maximum magnitude value is. The confidence limits equation (probabilities) known as the fiducial distribution is given by (Kijko, 2004):

$$\mathrm{P_r}[m_{max} < z] = 1 - [F_M(m_{max}^{obs}; z)]^n \tag{5.1}$$

where $F_M(m;\bullet)$denotes the cumulative density function of parameter m_{max}, z correspond to any value less than m_{max}, n is the number of seismic events and $m_{max}^{obs}$is the maximum observed magnitude.

The probabilities (confidence limits) for K-S, K-S-B and N-P-G procedures are ≈ 0.12, 0.28 and 0.61, respectively. According to Pisarenko (1991), the assessment of m_{max} is reliable and stable when the confidence limit is equal to 0.90 or higher. As a result, estimators of m_{max} following procedures developed by K-S, K-S-B and N-P-G do not seem to fit the magnitude distribution of the Mt. Cameroon Volcano region. However, the N-P-G procedure is more reliable and useful

than the model-based estimator K-S and K-S-B since it does not require any specification about the magnitude distribution function $F_M(m)$ (Kijko, 2004).

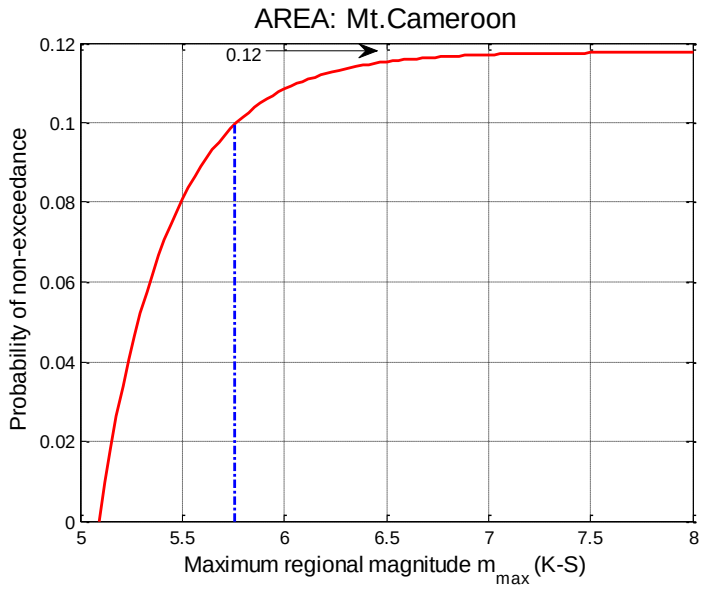

Figure 5.5: Fiducial distribution function of m_{max} for Mt. Cameroon when the Gutenberg-Richter model of the earthquakes magnitude is assumed. The value of m_{max} calculated according to the K-S procedure and its confidence limit are represented by the dash

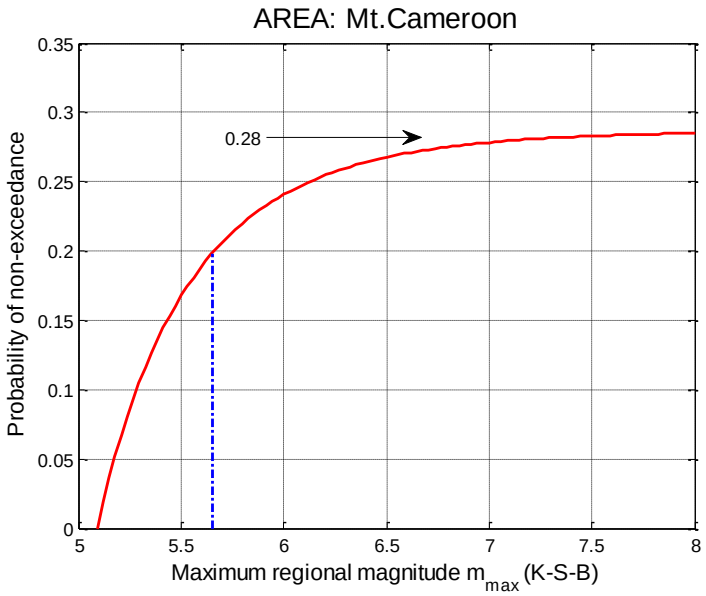

Figure 5.6: Fiducial distribution function of $\boldsymbol{m_{max}}$ for Mt. Cameroon when the Gutenberg-Richter-Bayes (K-S-B) model of the earthquakes magnitude is assumed. The value of $\boldsymbol{m_{max}}$ and its confidence limit are represented by the dashed vertical line and the arrow respectively.

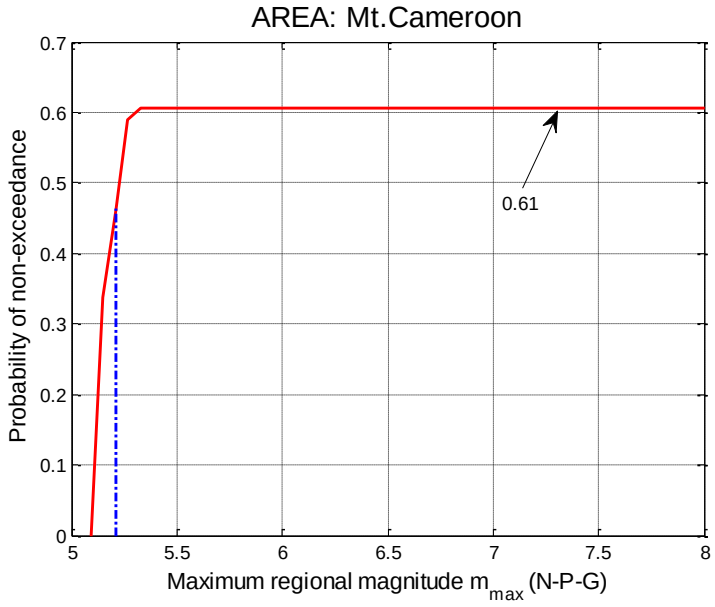

Figure 5.7 Fiducial distribution function of m_{max} for Mt. Cameroon when the empirical distribution of magnitude is estimated according to the N-P-G procedure. The value of m_{max} is equal to 5.21 and the probability defining whether the model is suitable to assess the value of m_{max} is equal to 0.61

The very low values of the confidence limits for K-S, K-S-B and N-P-G procedures can be attributed to the short period of observations of our seismic data (84 years). Pisarenko (1991) noticed that the span of a seismic catalogue is generally considered to be sufficient if the catalogue contains a minimum of two to three earthquakes with magnitude close to m_{max} (with a difference of order of 0.3 to 0.4).

The maximum magnitude estimated from the N-P-G procedure is equal to 5.21; The three largest earthquakes that took place in the Mt. Cameroon area are of moment magnitude 5.09, 4.95 and 4.75; only two magnitude values (5.09 and 4.95) are close to the values obtained from non-parametric estimators and none of them is close to the parametric estimators values (cf. Table 5.2). This implies that estimators based on the Gutenberg-Richter model may not be valid for the Mt. Cameroon region.

However, parametric approaches have the major advantage of being able to incorporate additional geological or geophysical information to supplement the pure seismological data. Therefore, they provide an appropriate tool that takes uncertainties into account (Kijko & Graham, 1998).

It should be noted that the estimated standard errors of the maximum possible magnitudes m_{max} depend on the chosen errors of maximum observed magnitude, which was arbitrary taken to be

0.3 in this study. Also, not considering the uncertainties resulting from a selection of the wrong magnitude distribution model can produce unacceptably erroneous estimations of m_{max} (Kijko and Graham, 1998).

5.2 Evaluation of volcanic hazard at Mt. Cameroon volcano

A geostatistical study done by Lapi et al. (2010) suggests that the series of Mt. Cameroon eruptions are indefinitely random and independent of one another. These findings make the application of a Poisson distribution suitable to estimate the eruption rate of Mt. Cameroon Volcano. The knowledge of the parameter λ evaluated in Chapter 4 (section 4.3.2) allows us to estimate the volcanic risk, i.e. the probability to have an eruption in the next t years (Fig. 5.8). This is given by the formula

$$P(t) = 1 - e^{-\lambda t} \tag{5.2}$$

In other words, the probability for an eruption to occur is equal to one minus the probability not to have an eruption in the next t years. At the origin time (t = 0, taken to be the year 2015), the probability is zero. The mean recurrence time (1/ λ) of Mt. Cameroon is approximately 13 years. This value is slightly higher than the one from Lapi et al.; (2010) who found that the average rate of occurrence of Mt. Cameroon eruptions is approximately one every 10 years.

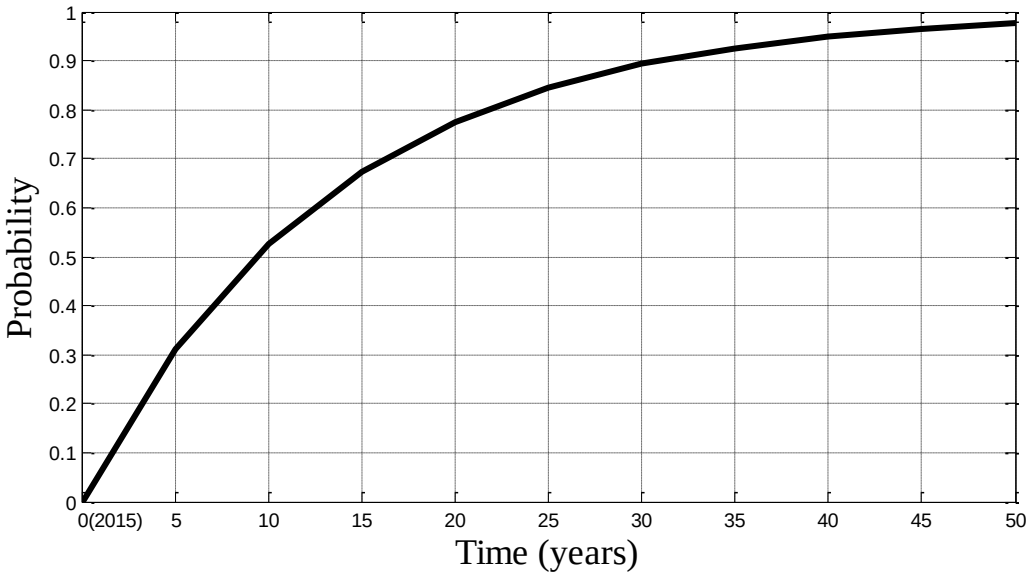

Figure 5.8: Probabilities for an eruption to occur in the next 50 years' time starting in the year 2015.

Considering the last eruption date (in 2000) and, with eruptions occurring once every 13 years, it is assumed that at present (2016) there is a high probability of eruption at Mt. Cameroon. In

general, there is a 52% chance for an eruption to occur before the end of the year 2025 and a 90% chance of eruption in the next 30 years (year 2045).

Geostatistical studies of Mt. Cameroon Volcano (Lapi et al., 2010) suggest that the next volcanic eruption at Mt. Cameroon is likely to take place in 2022. From our statistical assessment technique, there is only a 40 % chance of an eruption to occur in that year.

The volcanic risk evaluation of Mt. Cameroon from statistical methods used requires knowledge of the total number of eruptions during the observation period. Volcanic eruptions that occurred prior to1900 were used in the calculations even though there is no proven historical record about the exact occurrence dates (Deruelle et al., 1987). The traditional K-Ar dating technique usually contains large errors in the age range recorded by volcanoes (Ho et al., 1991). Thus, the exact duration of volcanism of Mt. Cameroon is still unknown. Also, the quality of results of statistical techniques depends on the length of the sample size (Ho et al., 1991). For a given volcano, the eruption history covering a long period of time yield reliable long-term average recurrence rate with precision. Records of eruptions at Mt. Cameroon are found back to 2500 B.C. (Deruelle et al., 1987), few of its eruptions have been documented. This is in great contrast to other volcanoes like Mount Etna whose documented eruption history dates back to more than 2500 years (Smethrurst et al., 2009). All these factors can influence the value of the mean annual recurrence rate and misestimate the risk of volcanism at Mt. Cameroon.

Chapter 6

Conclusion

This study has illustrated the feasibility of combining historical with instrumental seismic data and has produced some significant results on the seismicity and eruptions pattern of Mt. Cameroon. Nevertheless, as any hazard and risks assessment, the reliability of the results for a given area depends on the methodology and the input information used. Compare with any other unbiased estimator, the maximum likelihood procedure provides more robust and straightforward estimates with the least uncertainty.

6.1 Summary of the results

An examination of the Gutenberg-Richter Frequency magnitude (Fig. 4.4-4.6) shows that *b*-values are partially dependent on the maximum regional magnitude and the method used in their calculation. Also, *b*-values vary both temporally and spatially with an average value of 1.53 ± 0.02 estimated for the Mt.Cameroon region. This value is typical for volcanic areas where *b*-values are usually greater than one. We interpreted this anomalous *b*-value as the presence of high material heterogeneity beneath Mt. Cameroon. The intrusion of the magma body generates the occurrence of relatively small earthquakes as observed in our instrumental catalogue and could be responsible for the high *b*-values.

The great majority of sub-crustal earthquakes recorded reveal that the southeast zone is the most seismically active part of Mt. Cameroon volcano. By splitting our instrumental sub-catalogue into two (Table 5.1), we observed that the annual mean seismic activity rate strongly depends on the time span of the seismic catalogue and results show that on average, one earthquake event occurs every 10 days.

The maximum regional magnitude values determined from various approaches overlap with each other when their standard deviations are considered. However, the non-parametric with Gaussian Kernel (N-P-G) approach gave a more reliable maximum regional magnitude value. This may imply that the magnitude distribution model of the Mt. Cameroon earthquakes does not follow the form of the Gutenberg-Richter frequency magnitude relationship.

Since volcanic eruptions occurrence does not follow a specific pattern, a Poisson distribution was fitted to the previous recorded eruptions of Mt. Cameroon to estimate the rate of occurrence of volcanic eruptions and evaluate the risk of a future eruption. On average, one eruption takes place every 13 years and, with the last eruption occurring over 15 years ago, it is considered that there is at present a high probability of eruption.

The application of statistical techniques in volcanic areas require a sufficiently large sample size (time span of the seismic catalogue and number of volcanic eruptions) to evaluate a reliable prediction in the long run. An earthquake catalogue containing events for a period of time of just under 84 years and the fact that only 16 eruptions have been recorded so far do not give enough information to produce highly accurate results.

The seismic catalogue showed unusual inconsistencies such as having gaps, for example, from mid-1986 up to early 1987. This could be attributed to the downtime of the seismic network. Since an assumption has to be made that the instrumental data is complete, this considerably increases uncertainties in the values of the seismic hazard parameters. Likewise, the precise eruptions history of a volcano is not always known. Thus, to a certain extend, volcanoes are inherently unpredictable and this study only serve to provide average estimates of hazard and risks calculations. Nevertheless, as weather forecasting, it is much better to have forecast with known limitation (probabilities, uncertainties) than none at all.

Precise dates of eruptions are critical for volcanic rate calculations. The commonly used K-Ar dating method often has large errors in the age and duration of volcanism. Therefore, a more precise technique of dating is needed and the record of past volcanic eruptions of Mt. Cameroon must be developed by detailed field and geochronologics studies

6.2 Suggestions for Further Work

Admittedly, because of time and data availability constraint, this study has not been exhaustive and many of the lines of investigation pursued can still be extended considerably.

The reliability of the results for seismic hazard estimation in a given region depends on the methodology and input information used. In this thesis, we have applied a MLM to a combination of disparate catalogues covering about 84-years long seismic data. This period is not considered long enough and more recent seismic data should be added to produce highly accurate results.

The hazard parameters λ, m_{max} and b-value represent the seismic potential of a zone and attention should be focused on these parameters. For instance, with additional seismic data and better broadband seismograph coverage, the resolution in the determination of the focal depth of earthquakes will be improved. This will allow better determinations of the b-value distribution both laterally and with depth as well as over time. This technique has found applications to many geological problems, including the determination of the magma chamber location, size, and morphology (Gridges and Gao, 2007; Sánchez et al., 2005).

This study has demonstrated the feasibility of the technique developed by Kijko & Sellevoll (1989, 1992) in a volcanic environment. A necessary improvement would be in the assessment of the *b*- value and seismic activity rate. For example, instead of taking one average value for the whole region, a similar technique could be used to calculate these seismic parameters at each grid point. This will help delineate zones of lower earthquake risk where human settlement should preferably be located.

References

Aki, K. 1965. Maximum Likelihood estimate of *b* in the formula log *N* = *a-bM* and its confidence limits, *Bulletin of the Earthquake Research Institute*, Vol. 43, pp.237-239.

Ambey, W.B. and Fairhead, J.D., 1991. Regular, deep seismicity beneath Mt.Cameroon volcano: lack of evidence for tidal triggering. *Geophysical Journal International*, Vol. 106, pp. 287-291.

Ambey, W.B., 1989. Seismicity and Seismological Studies of Mount Cameroon, West Africa, Ph.D thesis, *University of Leeds* (unpublished), 237 pp.

Ambey, W.B., Fairhead, J.D., Francis, D.J., Nnange, J.M., Djallo, S., 1989. Seismicity of the Mount Cameroon region, West Africa, *Journal of African Earth Sciences*, Vol. 9, pp. 1-7.

Ambraseys, N.N. and Adams, R.D. (1986) Seismicity of West Africa. *Annales Geophysicae*. Vol. 4, pp. 679-702.

Anonymous, 1910. Volcanic Eruption in the Kamerun, *Geographical Journal*, Vol. 36, No. 1, pp. 103-104.

Ateba, B., Dorbath, C., Dorbath, L., Ntepe, N., Frogneux, M., Aka, F.T., Hell, J.V., Delmond, J.C., Manguelle, D., 2009. Eruptive and earthquake activities related to the 2000 eruption of Mount Cameroon volcano (West Africa), *Journal of Volcanology and Geothermal Research*, Vol. 179, pp. 206-216.

Ateba, B., Ntepe, N., Ekodeck, G.E., Soba, D., Fairhead, J.D., 1992. The recent earthquakes of South Cameroon and their possible relationship with main geological features of Central Africa, *Journal of African Earth Sciences*, Vol. 14, No. 3, pp. 365-369.

Benjamin, J.R., and Cornell, C.A. 1970. *Probability, Statistics, and Decision for Civil Engineers*. New York: McGraw-Hill.

Benkhelil, J., 1989. The origin and the evolution of the Cretaceous Benue Trough (Nigeria), *Journal of African Earth Sciences*, Vol. 8, No. 2, pp. 251-282.

Bikoro, B.-A. M., Ndougsa, M. T., Tabod, C.T., 2014. Quantitative interpretation of magnetic anomalies in Ebolowa-Njoum area (Southern Cameroon), *Geophysica*, Vol. 50, No. 1, pp. 11-25.

Caniaux, G., 2005. Analyse de la fréquence des eruptions volcaniques aus Açores: contribution a l'évaluation des risqué. *Bulletin de la Société Géologique de France*, Titre 176 (No. 1), pp. 107-120.

Captain Mateer, Waldau, G., Reading A.A. 1922, Volcanic Eruptions on the Cameroons Mountain, The *Geographical Journal*, Vol. 60, No. 2, pp. 135-141

Collignon, F., 1968. Gravimétrie de reconnaissance de la République Fédérale du Cameroun, *ORSTOM*, Paris, pp. 35.

Consul, P.C., 1989, Generalized Poisson Distributions: properties and Application, MARCEL DEKKER, INC New York, 300pp.

Cooke, P. 1979, Statistical inference for bounds of random variables, *Biometrika*, Vol. 66 (2), pp 367-374.

Cornell, C. A. (1994). Statistical Analysis of Maximum Magnitudes. In Johnston, A. C., Coppersmith, K. J., Kanter, L. R., & Cornell, C. A. (Editors), The Earthquakes of Stable Continental Regions - Vol. 1. Assessment of Large Earthquake Potential. California, *Electric Power Research Institute, Palo Alto,* p. 5–1 - 5–27.

Cramér, H. 1961. Mathematical Methods of Statistics, 2nd Edition, Princeton University Press: Princeton.

De Swardt, A.M.J., 1956. The 1954 Eruption of Cameroon Mountain, *Geological Survey of Nigeria Bulletin*, Vol. 1954, pp. 35-40.

Déruelle, B., Bardintzeff, J.M., Cheminée, J.L., Ngounouno, I., Lissome, J., Nkoumbou, C., Etamé, J., Hell, J.V., Tanyileke, G., N'ni, J., Ateba, B., Ntepe, N., Nono, A., Wandji, P., Fosso, J., Nkouathio, D.G., 2000. Eruption simultanées de basalte alcalin et de basalte alcalin et de hawaiite au Mont Cameroun. 28 Mars-17 Avril 1999, Comptes rendus de l'Académie des Sciences, *Serie II. Sciences de la terre et des Planètes*, Vol. 331, No 8, pp. 525-531.

Déruelle, B., Moreau, C., Nkoumbou, C., Kambou, R., Lissom, J., Njonfang, E., Ghogomu, R.T., Nono, A., 1991. The Cameroon Line: a review, in Kampunzu, A.B., Lubala, R.T. (Eds.), Magmatism in extensional structural settings. *The Phanerozoic African Plate, Springer-Verlag*, pp. 274-327.

Déruelle, B., N'ni, J., Kambou, R., 1987. Mount Cameroon: an active volcano of the Cameroon Line, *Journal of African Earth Sciences*, Vol. 6, pp. 197-214.

Dwight, H.B., 1961. Tables of Integrals and Other Mathamatical Data, 3rd ed., Macmillan Co., New York.

EERI Committee on Seismic Risk, (H. C. Shah, Chairman), (1984). Glossary of Terms for Probabilistic Seismic Risk and Hazard Analysis. *Earthquake Spectra*, 1: 33-36

Fairhead, J.D. (1985). Preliminary study of the seismicity associated with the Cameroon Volcanic Province during the volcanic eruption of Mt. Cameroon in 1982. *Journal of Africa Earth Sciences*, Vol. 3, pp 197-301.

Favalli, M., Tarquini, S., Papale, P., Fomaciai, A., Boschi, E., 2012. Lava flow hazard and risk at Mt. Cameroon volcano. *Bulletin of Volcanology*, Vol. 74, pp. 423-439.

Feumoe, A.N.S., Ndougsa, M.T., Manguelle, D.E., Fairhead, J.D., 2012. Delineation of tectonic lineaments using aeromagnetic data for the south-east Cameroon area, *Geofizika*, Vol. 29, No. 2, pp. 175-192.

Fitton, J.G., 1980. The Benue Trough and Cameroon Line – a Migrating rift system in west Africa, *Earth and Planetary Science Letters*, Vol. 51, pp. 132-138.

Fitton, J.G., Kilburn, C.R.J., Thirhvall, M.F., Hugues, D.J., 1983. 1982 Eruption of the Mount Cameroon, *West Africa, Nature*, Vol. 306, pp. 327-332.

Geze, B. 1953. Les Volcans du Cameroun Occidental, *Bulletin Volcanologique*, Vol. 13, 63–92.

Gibowicz, S.J. and Kijko. A. (1994) An introduction to mining seismology, *Institute of Geophysics, Polish Academy of Sciences, Warsaw, Poland,* 385 p

Gridges, D.L. and Gao, S.S. (2007) Spatial variation of seismic *b*-values beneath Makushin Volcano, Unalaska Island, Alaska, *Earth and Planetary Science Letters*, Vol. 245, pp. 408-415

Guillaume, G.M.D., 1966. Notes on the Cameron mountain, Buea, *Printed by the Government Printer* Buea, 22pp.

Gupta, H (2011), Introduction to Probabilistic Seismic Hazard Analysis (Extended version of contribution by A. Kijko). Encyclopaedia of Solid Earth Geophysics, Harsh Gupta (Editor). *Springer*.

Gupta, I.D., 2002, The state of the art in Seismic Hazard Analysis, *ISET Journal of Earthquake Technology*, Vol, 39, No.4, pp 311-346.

Gutenberg, B. And Richter, C.F. 1944. Frequency if earthquakes in California, *Bulletin of the Seismological Society of America*, Vol. 34, No. 4, pp. 185-188.

Gutenberg, B. And Richter, C.F. 1954. *Seismicity of the Earth*, Second Ed., Princeton University Press, New Jersey, 310pp.

Habermann, R.E., 1987. Man-Made changes of Seismicity rates, *Bulletin of the seismological Society of America.* Vol., 77, No. 1 pp.

Haight, Frank.A.,1967, handbook of the Poisson distribution, John Wiley &Sons, Inc. 168pp

Hanks, T. and Kanamori, H. (1979) A moment magnitude scale, *Journal of Geophysical Research*, Vol. 84, pp. 2348-2350.

Jennings, J.H. 1959. The eruption of Mount Cameroon February – March 1959. Geography Journal. Vol. 4, 207-208

Jones, G., Chester, D.K., Shooshtarian, F., 1999. Statistical analysis of the frequency of eruptions at Furnas Volcano, São Miguel, Azores, *Journal of Volcanology and Geothermal Research*, Vol. 92, pp. 31-38.

Joyner, B.W. (1984) A scaling law for the spectra of large earthquakes. *Bulletin of the Seismological Society of America*, Vol. 74, pp. 1167-1188.

Kijko, A. and Graham, G. 1999. "Parametric-historic" Procedure for Probabilistic Seismic Hazard Analysis, Part II: Assessment of Seismic Hazard at Specific Site, *Pure and Applied. Geophysics*, Vol. 154, pp. 1-22.

Kijko, A. and Graham, G. 1999. Parametric –historic Procedure for Probabilistic Seismic Hazard Analysis, Part I: Estimation of Maximum Regional Magnitude $m_{\max}$, *Pure and Applied Geophysics*, Vol. 152, pp. 413-442.

Kijko, A. and Sellevoll, M.A., 1989. Estimation of earthquake hazard parameters from incomplete data files. Part I. Utilization of extreme and incomplete catalogs with different threshold magnitudes, *Bulletin of the Seismological Society of America*, Vol. 79, No. 3, pp. 645-654.

Kijko, A. and Sellevoll, M.A., 1992. Estimation of earthquake hazard parameters from incomplete data files. Part II. Incorporation of magnitude heterogeneity, *Bulletin of the Seismological Society of America*, Vol. 82, No. 1, pp. 120-134.

Kijko, A. and Singh, M. 2011. Statistical Tools for Maximum Possible Earthquake Magnitude Estimation, *Acta Geophysica*, Vol. 59, No. 4, pp. 674-700, DOI: 10.2478/s11600-011-0012-6.

Kijko, A. and Smit, A., 2012. Extension of the Aki-Utsu *b*-Value Estimator for Incomplete Catalogs, *Bulletin of the Seismological Society of America*, Vol. 102 No. 3, pp. 1283-1287.

Kijko, A., 2004. Estimation of the Maximum Magnitude, $m_{\max}$, *Pure and Applied Geophysics*, Vol. 161, pp. 1-27, DOI: 10.1007/s0024-004-2531-4.

Klein, F.W., 1982.Patterms of historical eruptions at Hawaiian volcanoes, Journal of Volcanology and Geothermal Research, Vol. 12, pp. 1-35.

Lapi, P.N., Ofoma, A.E., Amobi, J.O., Ngah, S.A., Chiaghanam, O.I., 2010. Geostatistical Prediction of Future Volcanic Eruption and Risk Assessment for the Mount Cameroon Volcano, Global Journal of Pure and Applied Sciences, Vol., 16, No. 1, pp. 115-128.

Marshall, P.D. (1970) Aspect of spectral differences between earthquakes and underground explosions, *Geophysical Journal of the royal Astronomical Society*, Vol. 20, pp. 397-416.

Mavonga, T., Zana, N., Durrheim, R.J., 2010. Studies of crustal structure, seismic precursors to volcanic eruptions and earthquake hazard in the eastern provinces of the Democratic Republic of Congo, *Journal of African Earth Sciences*, Vol. 58 No. 4, pp. 623-633.

Mc.Nuti, S.R. (2005). Volcanic Seismology, *Annu. Rev. Earth Planet Science*, Vol. 32, pp. 461-491.

McGuire, R. M. (1993), Computation of Seismic Hazard, *Annali Di Geofisica*, 36 (3-4): 181–200.

Mignan, A., J. Woessner (2012), Estimating the magnitude of completeness for earthquake catalogs, Community Online Resource for Statistical Seismicity Analysis, doi:10.5078/corssa-00180805. Available at http://www.corssa.org

Montigny,R., Ngounouno, I., Déruelle, B. 2004 Âges K-Ar des roches magmatiques de fosséde Garoua (Cameroun): leur place dans le cadre de la «Ligne du Cameroun», *Comptes Rendus de Geoscience*, Vol. 336, pp. 1493-1471.

Ndikum, E.N., Tabod. C.T., Tokam, A.-P.K., Essimbi, B.Z., 2014. Fault-plane solution of the earthquakes of 19 March 2005 in Monatele. *Open Journal of Geology*, Vol. 4, 289-293.

Ndougsa, M.T., Yufenyiu, L.D., Yene, A.J.Q., Tabod, C.T., 2014. Delineation of the northern limit of the Congo Craton based on spectral analysis and 2.5D modelling of aeromagnetic data in the Akonolinga-Mbama area, Cameroon, *Geofísica Internacional*, Vol. 53, No. 1, pp. 5-16.

Ngwa, C.N., Suh, C.E., Devey, C.W., 2010. Phreatomagmatic deposits and stratigraphic reconstruction at Debunscha Maar (Mt Cameroon volcano), *Journal of Volcanology and Geothermal Research*, Vol. 192, pp. 201-211.

Njome, M.S., Suh, C.E., Chuyong, G., de Wits, M.J., 2010. Volcanic risk perception in rural communities along the slope of mount Cameroon, West-Central Africa, *Journal of African Earth Sciences*, Vol. 58, pp. 608-622.

Nkoumbou, C., Deruelle, B., Velve, D., 1995. Petrology of Mt. Etinde Nephelinite Series, *Journal of Petrology*, Vol. 36, No. 2, pp. 373-393.

Nnange, J.M., Ngako, V., Fairhead, J.D., Ebinger, C.J, 2000. Depths density discontinuities beneath the Adamawa Plateau region, from spectral analyses of new and existing gravity data, *Journal of African Earth Sciences*, Vol 30, No. 4, pp. 887-901.

Ntepe, N., Aka, F.T., Ubangoh, R.U., Ateba, B., Nnange, J.M., Hell, J.V., 2004. The July 2002 earthquakes in the Kribi region: geological context and a preliminary evaluation of seismic risk in southwestern Cemeroon, *Journal of African Earth Sciences*, Vol. 40, pp. 163-172.

Okereke, C.S., Fairhead, J.F., 1984. A catalogue of gravity measurements for Nigeria and Cameroo, Department of Earth Sciences, *University of Leeds*, 300 pp.(unpublished)

Page, R., 1968. Aftershocks and Microaftershocks of the great Alaska Earthquakes of 1964, *Bulletin of the Seismological Society of America*, Vol. 58 No. 3, pp. 1131-1168.

Piper, J.D. and Richardson, A., 1972. The Paleomagnetism of the Gulf of Guinea Volcanic Province, West Africa, *Geophysical Journal of Royal Astronomy Society*, Vol. 29, pp. 147-171.

Pisarenko, V.F., 1991. Statistical Evaluation of Maximum Possible magnitude, Izvestiya Earth Physics, Vol. 27, pp. 757-763.

Pisarenko, V.F., Lyubushin, A.A., Lysenko, V.B., Golubeva, T.V., 1996. Statistical Estimation of Seismic Hazard Parameters: Maximum Possible and related Parameters, *Bulletin of the Seismological Society of America,* Vol. 86, No. 3, pp. 691-700.

Plomerová, J., Babuska, V., Dorbath, C., Dorbath, L., Lillie, R.J., 1993. Deep lithospheric structure across the Central African Shear Zone in Cameroon, *Geophysical Journal International*, Vol.115, pp.381-390

Poudjom, D.Y.H.,Nnange, J.M., Diament, M., Ebinger, C.J., Fairhead, J.D., 1995. Effective elastic thickness and crustal thickness variations in west central Africa inferred from gravity data, *Journal of Geophysical Research*, Vol. 100, No. B11, pp. 22047-22070.

Richter, C.F. (1958) Elementary seismology, *Freeman and Co., San Francisco, United States of America*, pp. 364-367.

Richter, C.F., 1935. An Instrumental Earthquake magnitude Scale, *Bulletin of the Seismological Society of America*, Vol. 25, No. 1, pp. 1-32.

Rydelek, P. A. & Sacks, I. S. (1989). Testing the completeness of earthquake catalogs and the hypothesis of self-similarity, *Nature*, 337(6204): 251– 253. DOI: 10.1038/337251a0.

Sánchez, J.J., Gómez, D.M., Torres, R. A, Calvache, M.L., Ortega, A., Ponce, A.P., Acevedo, A.P., Gil-Cruz, F., Londono, J.M., Rogriguez, S.P., Patino, J.De J., Bohorquez, O.P. (2005). Spatial Mapping of the *b*-value at Galeras Volcano, Colombia, Using Earthquakes Recorded from 1995 to 2002, *Earth Sciences Research Journal*, Vol. 9, No. 1 pp. 30-36.

Schlüter, T., 2008. Geological Atlas of Africa with notes on Stratigraphy, Tectonics, Economy Geology, Geohazards, Geosites, and Geoscientific education of each country, *Spinger- Verlag Berlin Heidelburg*, 307 p

Schorlemmer, D., and Woessner J., 2008. Probability of detecting an earthquake, *Bulletin of the Seismological Society of America*, Vol. 98, No pp. 2103-2117

Scordidis, E.M., 2006. Empirical global relations converting M_S and m_b to moment magnitude, *Journal of Seismology*, Vol. 10, pp. 225-236.

Sereno, T.J.Jr. and Bratt, S.R., 1989. Seismic Detection Capability at NORESS and Implications for the Detection Treshold of a Hypothetical Network in the Soviet Union, *Journal of Geophysical research*, Vol. 94, No. B8, pp. 10397-10414.

Singh, K.S., Ordaz, M., Lindholm, C.D., Havskov, J., 1990. Seismic Hazard in southern Norway, *Bergen University seismology Series*, Vol. 46, pp. 1-33.

Smethrust, L., James, M.R., Pinkerton, H., Tawn, J.A., 2009. A statistical analysis of eruptive activity on Mount Etna, Sicily, *Geophysical Journal International*, Vol. 179, pp. 655-666, doi: 10.1111/j.1365-246X.2009.04286.x

Sparks, R.S.J., 2003. Forecasting volcanic eruptions, *Earth and Planetary Science Letters*, Vol. 210, pp. 1-15.

Stuart, G.W., Fairhead, J.D., Dorbath, L., Dorbath, C., 1985. A seismic refraction study of the crustal structure associated with the Adamawa Plateau and the Garoua rift, Cameroon, West Africa, *Geophysical Journal of Astronomical Society*, Vol. 81, pp. 1-12.

Suh, C.E., Sparks, R. S. J., Fitton, J. G., Ayonghe, S. N., Annen, C., Nana,R., Luckman, A., 2003. The 1999 and 2000 eruptions of Mount Cameroon: eruptive behavior and petrochemistry of lava, *Bulletin of Volcanology*, Vol. 65, pp. 267-28.

Suh, C.E., Stansfield, S.A., Sparks, R.S.J., Njome, M.S., Wantim, M.N., Ernst, G.G.J., 2011. Morphology and structure of the 1999 lava flows at Mount Cameroon Volcano (West Africa) and their bearing on the emplacement dynamics of volume-limited flows, *Geological Magazine*, Vol. 148, No. 1, pp. 22-34.

Tabod, C.T., and Fairhead J.D., 1992. Seismicity of the Cameroon Volcanic line, *Tectonophysics*, Vol. 212, pp. 303-320.

Tate, R.F., 1959. Unbiased estimation: Functions of location and scale parameters, *Ann. Math. Stat*, Vol. 30, pp. 341-366.

Thierry, P., Stieltjes, L., Kouakam, E., Nguéya, P., Salley, P.M., 2008. Multi-hazard risk mapping and assessment on an active volcano: the GRINP project at Mount Cameroon, *Natural Hazards*, Vol. 45, pp. 429-456.

Tokam, A.-P, K., Tabod, C.T., Nyblade, A.A., Julià J., Wien, D.A., Paysanos, M.E., 2010. Structure of the Crust beneath Cameroon, West Africa, from the joint inversion of Rayleigh

wave group velocities and receiver functions, *Geohysical Journal International*, Vol. 183, Issue 2, pp. 1061-1076.

Toteu, S.F., Van Schmus, W.R., Penaye, J., Michard, A., 2001. New U-Pb and Sm- Nd data from north Cameroon and its bearing on the pre-Pan African history of central Africa, *Precambrian Research*, Vol. 108, pp. 45-73.

Ubangoh, R.U., Ateba, B., Ayonghe, S.N., Ekodeck, G.E., 1997. Earthquakes swarms of Mt. Cameroon, West Africa, *Journal of African Earth Sciences*, Vol. 24, No. 4, pp. 413-424.

Utsu, T., 1965. A method for determining the value of *b* in the formula log *n* = *a*-*bM* showing the magnitude –frequency relation for earthquakes, *Geophysical Bulletin of Hokkaido University*, Vol. 13, pp. 99-103 (in Japanese with English summary).

Wantim, M.N., 2011. Mapping and modelling Lava flow Dynamics and Hazards at Mount Cameroon Volcano, Ph.D thesis, Department of Geology and soil Science, *Ghent University*, 284 pp.

Ward, S. 1997, More on $M_{\max}$, *Bulletin of the Seismological Society of America*, Vol. 87, No. 5, pp. 1199-1208.

Wheeler, R.L., 2009. Methods of Mmax Estimation East of Rocky Mountains. USGS, Open-File Report, 2009-1018.

Wiemer, S, and Wyss, M. 2000. Methods of M_{max} estimation East of Rocky Mountains. (open-File Report 2009-1018). USGS: United States of America.

Wiemer, S. And Wyss M., 2000. Minimum Magnitude of Completeness in Earthquake Catalogs: Examples from Alaska, the Western United States, and Japan, *Bulletin of the Seismological Society of America*, Vol. 90, No. 4, pp. 859-869.

Woessner, J. And Wiemer, S. 2005. Assessing the Quality of Earthquakes catalogues: Estimating the Magnitude of Completeness and Its Uncertainty, *Bulletin of the Seismological Society of America*, Vol. 95, No. 2, pp. 684-698.

Zogning, A., 1988. Le Mont Cameroon, un volcan actif: contribution a l'étude de géographie physique appliquée, Thèse Doc. 3C, Univ. Yaoundé, 447 pp.